

APPLICATION OF THE METHOD OF
INTEGRAL RELATIONS TO THE CALCULATIONS
OF INCOMPRESSIBLE TURBULENT BOUNDARY LAYERS

By

John D. Murphy & William C. Rose*
NASA - Ames Research Center

INTRODUCTION

The present investigation was carried out to determine the efficiency and accuracy of a moment method as applied to the calculation of incompressible turbulent boundary layers. This method, at least conceptually, promises to be more accurate than the classical von Karman integral methods while requiring less computing time than previously employed finite difference methods.

The moment method employed in the present study is popularly known as the "method of integral relations", following Dorodnitsyn (1960). It is one of a family of methods that are known in the mathematics literature as Petrov's generalization of the Galerkin method (Mikhlin and Smolitskiy (1967)). Briefly, the mathematical procedure employed is to approximate the actual solution to a differential equation, where the solution is given by an infinite series (hence, the solution is said to lie in an infinite dimensional vector space). The approximation is taken in the form of a partial sum of the infinite series, thus placing the approximate solution in a finite dimensional vector space. This finite dimensional space is completely described by a system of coordinate vectors (normally referred

* Research Scientists

to in moment methods as "weighting functions") in that any element (e.g. the assumed solution) may be expressed as a linear combination of the coordinate vectors. The dimension of the subspace chosen to represent the solution is sometimes known as the "order of approximation", and is equal to the number of parameters which may be determined from use of the moment method.

The various moment methods used for solving the boundary layer equations basically differ only in the choice of these coordinate vectors and the form assumed for the approximate solution. The success of any moment method, then, depends on how well these choices can represent the actual solution. Several constructive theorems demonstrating exactness and convergence of general moment methods applied to non-linear equations have been given by Fetryshyn (1967).

Moment methods similar to that employed herein have been employed in the calculation of incompressible laminar boundary layers by Dorodnitsyn (1960) and Bethel and Abbott (1966) and to compressible laminar boundary layers by Pallone (1961), Pavlovskii (1962), Nielsen et al (1965), and Holt (1966). The adequacy of moment methods as applied to laminar flows has been demonstrated by these studies.

Deiwert and Abbott (1967) used a moment method with a three parameter velocity gradient profile together with empirical shear integrals, representing the turbulent transport mechanism, to solve the incompressible turbulent boundary layer equations. Through the use of empirical shear integrals determined from selected sets of data, they were able to predict the flow quantities for those particular sets of data, thus demonstrating the adequacy of the moment method applied in turbulent boundary layer flows.

In the present investigation, the results obtained using two, three, and four parameter velocity profiles were compared with flat plate data. It was found that the accuracy improved with increasing order of approximation. Based on these flat plate studies, it was felt that a four parameter velocity profile provided sufficient accuracy, and that higher parameter profiles would require excessive computing time. All of the results obtained in this study employed the four parameter profile. In order to provide a general procedure for predicting the behavior of the turbulent boundary layer with arbitrary free stream velocity variation, an eddy viscosity model was employed for the numerical evaluation of the shear integrals. A computing program was generated in this investigation and has been written so that any model of the turbulent transport mechanism may be easily incorporated. The results of this program are compared with the experimental data of sixteen turbulent flows. These flows are listed in table 1.

NOMENCLATURE*

$C_j(s)$	coefficients in approximate velocity gradient profile representation
$f_1(\hat{u}), g_1(\hat{u})$	weighting functions employed in equations (5) and (6)
INT_1	dissipation integrals defined in equation (10)
P, Q, R	exponents defined in equation (8)
s	transformed streamwise coordinate
\hat{u}	U/U_∞
α	exponent defined in equation (10)
λ	eigenvalue of linearized version of equation (10)
σ_1, σ_2	error magnitudes defined in equations (3a) and (4a)
ϕ	reciprocal normalized velocity gradient, $\partial y / \partial \hat{u}$

Superscript

\sim	denotes approximate functional representation
	Subscript
o	denotes quantities at initial station

*The uniform symbols suggested by Kline et al have been employed wherever possible. This table defines only those symbols which are not provided for in the uniform symbol tabulation.

ANALYSIS

The analysis given below differs in concept and procedure from those previously published. It is the authors' belief that the present analysis, while more complex mathematically, provides a clearer understanding of the operations employed, than do previous derivations.

The boundary layer equations for two-dimensional incompressible turbulent flow are written in Boussinesq form as:

$$-U \frac{\partial U}{\partial x} + v \frac{\partial U}{\partial y} - U_\infty \frac{dU_\infty}{dx} - \frac{\partial}{\partial y} \left[\left(1 + \frac{\epsilon}{\mu}\right) \nu \frac{\partial U}{\partial y} \right] = 0 \quad (1)$$

$$\frac{\partial U}{\partial x} + \frac{\partial v}{\partial y} = 0, \quad (2)$$

where $\epsilon = -\rho \overline{uv} / \partial U / \partial y$

The terms $\frac{\partial \overline{u^2}}{\partial x}$ and $\frac{\partial \overline{uv}}{\partial x}$ have been considered negligible in comparison with $\frac{\partial \overline{uv}}{\partial y}$.

Employing a change of variable: $\hat{u} = U/U_\infty$,

the Crocco transformation $x \rightarrow s(x)$, $y \rightarrow \hat{y}(x, y)$,

and setting $\phi = 1 / \frac{\partial \hat{u}}{\partial y}$,

we obtain from (1) and (2):

$$-\hat{u} \frac{\partial \hat{y}}{\partial s} + \frac{\hat{y}}{U_\infty} - (1 - \hat{u}^2) \frac{\phi}{U_\infty} \frac{dU_\infty}{ds} - \frac{1}{U_\infty} \frac{\partial}{\partial \hat{u}} \left[\left(1 + \frac{\epsilon}{\mu}\right) \frac{\hat{y}}{\phi} \right] = 0 \quad (3)$$

$$-\frac{\partial \hat{y}}{\partial s} + \frac{\phi \hat{u}}{U_\infty} \frac{dU_\infty}{ds} + \frac{1}{U_\infty} \frac{\partial \hat{y}}{\partial \hat{u}} = 0, \quad (4)$$

where the term $\frac{\partial V}{\partial s}$ is given by $\frac{\partial}{\partial s} \int_0^{\hat{u}} \phi d\hat{u}$ from the definition of ϕ .

As this point we have two partial differential equations in the two unknowns V and ϕ . These equations differ from (1) and (2) in that now one of the independent variables, (i.e. \hat{u}) assumes values in the finite interval $0,1$.

We now employ Kantorovich's technique to reduce the partial differential equations to ordinary differential equations by approximating the \hat{u} dependence of the unknowns V and ϕ . This approximation is accomplished by the generalized Galerkin procedure (see Kantorovich and Krylov (1964) and Mikhlin and Smolitskiy (1967)). In this procedure, it is assumed that the functional dependence on \hat{u} of the unknowns V and ϕ can be represented by partial sums of the form:

$$V \approx \tilde{V} = \sum_{i=1}^n a_i(s) \hat{u}^{i-1} \quad ; \quad \phi \approx \tilde{\phi} = \sum_{i=1}^n c_i(s) \hat{u}^{i-1}$$

respectively.

The significance of the transforms employed to obtain equations (3) and (4) now becomes evident. From the Weierstrass approximation theorem, it is clear that the chosen form of \tilde{V} and $\tilde{\phi}$ can be made to respectively represent V and ϕ as accurately as one desires on the closed interval $0,1$. If we now substitute the approximate values of ϕ and V , i.e., $\tilde{\phi}$ and \tilde{V} , into equations (3) and (4) we obtain:

$$-\hat{u} \frac{\partial}{\partial s} \int_0^{\hat{u}} \tilde{\phi} d\hat{u} + \frac{\tilde{V}}{U_\infty} - \frac{\tilde{\phi}}{U_\infty} (1 - \hat{u}^2) \frac{dU_\infty}{ds} - \frac{1}{U_\infty} \frac{\partial}{\partial \hat{u}} \left[\left(1 + \frac{\epsilon}{\mu}\right) \frac{\tilde{V}}{\tilde{\phi}} \right] = \sigma_1 \quad (3a)$$

$$-\frac{\partial}{\partial s} \int_0^{\hat{u}} \tilde{\phi} d\hat{u} + \frac{\tilde{\phi} \hat{u}}{U_\infty} \frac{dU_\infty}{ds} + \frac{1}{U_\infty} \frac{\partial \tilde{V}}{\partial \hat{u}} = \sigma_2 \quad (4a)$$

where σ_1 and σ_2 differ from zero by virtue of the fact that approximate representations of ϕ and V have been introduced. We now require the errors σ_1 and σ_2 to be orthogonal to two linearly independent sets of coordinate vectors denoted by " f_1 " and " g_1 ", respectively. The form of f_1 and g_1 are given by:

$$\vec{f}_i(\hat{u}) = B \hat{u}^{i-1} \quad ; \quad \vec{g}_i(\hat{u}) = D \hat{u}^{i-1},$$

where B and D are arbitrary linear operators (c.f. Mikhlin and Smolitskiy (1967)). Invoking the infinite dimensional form of the inner product to impose the orthogonality condition over the domain $0 \leq \hat{u} \leq 1$, we obtain:

$$\int_{\hat{u}=0}^{\hat{u}=1} g_i \left[-\hat{u} \frac{\partial}{\partial s} \int_{\hat{u}=0}^{\hat{u}} \tilde{\phi} d\hat{u} + \frac{\tilde{V}}{U_\infty} - \frac{\tilde{\phi}}{U_\infty} \frac{dU_\infty}{ds} (1-\hat{u}^2) - \frac{1}{U_\infty} \frac{\partial}{\partial \hat{u}} \left[\left(1 + \frac{\epsilon}{\mu}\right) \frac{\tilde{V}}{\tilde{\phi}} \right] \right] d\hat{u} = 0 \quad (5)$$

$$\int_{\hat{u}=0}^{\hat{u}=1} f_i \left[-\frac{\partial}{\partial s} \int_{\hat{u}=0}^{\hat{u}} \tilde{\phi} d\hat{u} + \frac{\tilde{\phi} \hat{u}}{U_\infty} \frac{dU_\infty}{ds} + \frac{1}{U_\infty} \frac{\partial \tilde{V}}{\partial \hat{u}} \right] d\hat{u} = 0 \quad (6)$$

The inner product employed is a bi-linear operator so that (5) and (6) may be added and, upon carrying out the indicated operations and requiring that $g_1 = \frac{\partial \tilde{\phi}}{\partial \hat{u}}$ and $f_1(1) = 0$, written as;

$$\frac{d}{ds} \int_{\hat{u}=0}^{\hat{u}=1} \tilde{\phi} f_i \hat{u} d\hat{u} + \frac{1}{U_\infty} \frac{dU_\infty}{ds} \int_{\hat{u}=0}^{\hat{u}=1} \tilde{\phi} [f_i \hat{u} - f_i'(1-\hat{u}^2)] d\hat{u} - \frac{1}{U_\infty} \left\{ \frac{1}{\mu} \left(1 + \frac{\epsilon}{\mu}\right) \frac{\tilde{V}}{\tilde{\phi}} \right\}' \int_{\hat{u}=0}^{\hat{u}=1} f_i d\hat{u} + \frac{1}{U_\infty} \int_{\hat{u}=0}^{\hat{u}=1} f_i'' \left[\left(1 + \frac{\epsilon}{\mu}\right) \frac{\tilde{V}}{\tilde{\phi}} \right] d\hat{u} = 0 \quad (7)$$

where primes denote differentiation with respect to \hat{u} .

The choice of $\tilde{\phi}(\hat{u})$ is not arbitrary, but, rather, is restricted to functions satisfying the boundary conditions @ $\hat{u} = 0$ and $\hat{u} = 1$. One such $\tilde{\phi}$ is that which has been employed in laminar boundary layer studies:

$$\tilde{\phi} = \frac{1}{1-\hat{u}} \sum_{j=1}^n c_j(s) \hat{u}^{j-1}. \quad (8)$$

The form of the assumed velocity gradient profile, $\tilde{\phi}$, employed in the present study is:

$$\tilde{\phi} = \frac{1}{1-\hat{u}} [c_1(s) + c_2(s)\hat{u}^P + c_3(s)\hat{u}^Q + c_4(s)\hat{u}^R], \quad (8a)$$

where P, Q, and R are exponents assumed to be arbitrary for the moment.

The $f_i(\hat{u})$ chosen in the present study are:

$$f_i(\hat{u}) = (1-\hat{u})^i \quad i = 1, 2, 3, 4. \quad (9)$$

Substitution of (8a) and (9) into equation (7) and integration of the \hat{u} dependence yields a system of 4 ordinary non-linear differential equations in the four unknowns $C_j(s)$. These equations may be written in matrix form as:

$$[a_{ij}] \vec{C}_j = -\frac{\dot{U}_\infty}{U_\infty} [b_{ij}] \vec{C}_j + \frac{\nu \dot{U}_\infty}{U_\infty C_1} - \overline{INT}_i \quad (10)$$

where

$$a_{ij} = \int_{\hat{u}=0}^{\hat{u}=1} \hat{u}^i (1-\hat{u})^{j-1} d\hat{u}; \quad b_{ij} = \int_{\hat{u}=0}^{\hat{u}=1} (1-\hat{u})^{i-1} [\lambda^\alpha + i(1-\hat{u})\lambda^{\alpha-1}] d\hat{u},$$

for

j = 1	$\alpha = 1$
= 2	$= P+1$
= 3	$= Q+1$
= 4	$= R+1$

and

$$\overline{INT}_i = \frac{1}{U_\infty} \int_{\hat{u}=0}^{\hat{u}=1} \nu \left(1 + \frac{\hat{u}}{L_1}\right) \frac{i(i-1)(1-\hat{u})^{i-2}}{\tilde{\phi}} d\hat{u};$$

The "dot" denotes differentiation with respect to "s". It should be noted that $INT_1 = 0$ and it can be shown that $INT_2 = \frac{D}{\rho U_\infty^2}$

where D is the dissipation integral. The integrals INT_3 and INT_4 are moments of the integrand of the dissipation integral.

These are the equations programmed and solved in the present study. Once these equations are solved for the C_j , all of the boundary layer parameters of interest can be obtained by algebraic relations or simple quadratures.

DISCUSSION OF METHOD

General

Two general conclusions can be deduced from equation (7). First, in application to the present formulation, it is clear that an arbitrary number of computing equations can be generated by choosing a sufficient number of linearly independent weighting functions. Therefore, solutions for an arbitrary number of coefficients in equation (8) may be obtained. Second, and more generally, it can be seen that a whole family of computational methods are embodied in equation (7). If for example, a large number of square wave weighting functions were employed, and some variation of \hat{u} with y were assumed over each increment, a finite difference formulation could be obtained. This correspondence between the generalized moment methods and finite difference methods was recognized by Dorodnitsyn (1960) and also pointed out by Kendall and Bartlett (1967). Similarly if a combined law of the wall and law of the wake were assumed for the velocity profile and $f_1(\hat{u}) = 1$, for $0 \leq \hat{u} \leq 1$, and $f_2(\hat{u}) = 1$ for $0 \leq \hat{u} \leq 1/2$, a computing scheme similar to that employed by

Moses (1964) would be obtained.

In the present method the coordinate vectors are chosen to be continuous over the entire region $0 \leq \bar{u} \leq 1$ which eliminates the need of establishing "internal" boundary conditions.

The resulting system of non-linear ordinary differential equations may be integrated in the streamwise direction once the initial values of the C_j are chosen. This choice of the initial C_j has proven to be a particularly difficult problem. To determine the C_j representing experimental velocity profile at the initial station, two procedures were considered. The first procedure employed was to match the experimental values C_f , δ^* , θ , and kinetic energy thickness, δ_3 . It was found that small perturbations in the values of integral thickness parameters produced large excursions in the values of the C_j . This difficulty led to a second procedure in which C_f was matched and the predicted profile was made to pass through three data points in the initial experimental velocity profile. This procedure was found to yield satisfactory results for the integral parameters and was employed in the present study. Since no clear rules for choosing the three velocity profile points have been established a trial and error procedure must be employed. To obtain initial conditions, it was found however that, independent of the choice of points to be matched, any set of C_j yielding a good fit to the initial profile converged rapidly to a solution yielding the same physical parameters.

Choice of $\hat{\phi}$ and f_1

The forms chosen for the weighting functions and the velocity gradient profile ($\hat{\phi}$) are given in the preceding section. Both of these choices were

made on the basis of the success obtained using similar functions in laminar flow analysis. The success of the method depends on how well the approximate solution assumed represents the actual solution sought (i.e., how rapidly the infinite series representing the actual solution converges) and in addition on how well the assumed solution can be resolved in the subspace defined by the weighting functions. This latter point has not previously been clearly enunciated by investigators applying the method to boundary layer flows. In fact when the function chosen for $\hat{\psi}$ contains powers of \hat{u} not contained in the set of weighting functions, as in the present study and in Deiwert and Abbott (1967), an additional approximation is introduced. That is, the assumed solution does not lie wholly within the subspace defined by the weighting functions. Since the solution to the ordinary differential equations is, in fact, obtained in this subspace, only that portion of the initial profile which lies in the subspace may be resolved in subsequent computations. When the representation for $\hat{\psi}$ is so chosen, it is no longer possible to rigorously demonstrate exactness and convergence of the general moment method.

In the present study the weighting functions contain terms up to \hat{u}^3 . It was found, however, that to represent the spectrum of profiles required in the present study, see figure 1, sequentially complete polynomials of order three were inadequate. In particular, it was found that in order to generate the sharply inflected velocity profiles characteristic of favorable and zero pressure gradient flows large exponents must be chosen for the $\hat{\psi}$ representation ($P = 2, Q = 4, R = 6$). This choice of exponent was made for all flows represented in table 1 with the exception of the Tillmann flow ID 1500, and the Newman flow ID 3500. For the Tillmann flow, in order to obtain

correct initial conditions, the exponents have to be chosen as $P = 1$, $Q = 2$, $R = 3$. In order to determine the effects of the choice of exponents in the $\bar{\psi}$ representation a parametric study was carried out using the Newman flow as reference. Figure 2a shows a comparison of the results obtained for the exponents, $P = 1$, $Q = 5$, $R = 9$ and the exponents $P = 1$, $Q = 2$, $R = 3$ with the data of Newman (ID 3500). Five additional computer runs were made covering the intervening range of exponents and it was found that, as the highest exponent decreased, at the last station, the skin friction coefficient decreased monotonically, and the value of H increased monotonically. The momentum thickness, on the other hand, was essentially invariant with exponent choice and was in reasonable agreement with the data for all seven sets of computations. It should be noted that the initial values ($x_0 = 2.759$ feet) of the integral parameters and skin friction were well represented by all the sets of exponents considered. It is clear from consideration of figure 2b that for the experimental velocity profile obtained by Newman at station "C", low order exponents must be employed. It is equally clear that none of the exponents considered yield profiles which adequately describe the experimental results. Further discussion of this point is deferred to the section entitled Discussion of Results.

Choice of Eddy Viscosity Model

The eddy viscosity model employed in this study is that of van Driest (1956) for the wall region and that of Clauser (1956) for the wake region. These two models are simply patched together at equal values of ϵ . A slight variation from the van Driest model employed by Smith et al. (1965),

is used here in that the assumption of $\tau = \tau_w$ in the sublayer has not been made in this study. This model may be written as:

$$1 + \frac{\epsilon}{\mu} = 1.0 + 0.16 y^+ \left[1 - \exp(-y^+/20) \right] \left(\frac{24}{y^+} \right)$$

The Clauser Law is simply:

$$1 + \frac{\epsilon}{\mu} = 1.0 + 0.0168 Re_{\tau}^+ y^+$$

This choice of eddy viscosity model was made simply to permit a legitimate comparison of the results of the present method with the exact solutions of Smith et al. (1955). Such a comparison is shown in figure 3 for the flow of Schubauer and Klebanoff (ID 2100). It can be seen that both calculation procedures yield essentially the same results.

The basic moment method imposes no restrictions on the choice of eddy viscosity nor does it require the explicit formulation of an eddy viscosity model. This latter point is discussed in the following section.

Numerical Solutions

In an effort to make the present method comparable in machine time with the simpler integral methods an attempt was made to reduce the computation time involved in the streamwise integration. This can be accomplished by either reducing the number of integration steps required to traverse some fixed distance or by reducing the time required to take each step. Two methods of integration for the numerical solution of equation (10) were investigated and the time consumed by evaluation of the dissipation integrals was examined.

The first integration procedure employed was fourth order variable step size Adams-Moulton predictor-corrector integration routine. Secondly,

a modified-Euler implicit method employing local linearization of the derivatives was used. Lomax (1967) shows that the stability requirement implicit in fourth order Adams-Moulton integration is $|\lambda h| < 0.7$, where h is the integration stepsize and λ the largest eigenvalue of the locally linearized system. In order to avoid a small integration stepsize when parasitic eigenvalues are present (c.f. Lomax and Baily (1967)), the implicit Euler integration routine was employed. This latter integration scheme is stable for all $|\lambda h|$ but requires local linearization of the differential equations. The accuracy of the method is of $O(h)^3$ and the error in the linearization is of course $O(h^2)$ so that some limitation of stepsize is required to retain sufficient accuracy. In order to control the error, the simple expedient of permitting a maximum 1% variation in the most rapidly varying C_j was employed. It was found that a factor of two reduction in machine time could easily be obtained using the implicit integration. Table 1 compares IBM 7094 computation time for several sets of data for the two integration schemes.

The second item considered was the reduction of time required for each step. It was found that roughly 70 percent of the time required for each step was associated with the evaluation of the dissipation integral and its moments, (i.e., the INT_1). Deiwert and Abbott (1967) employed correlations of these integrals deduced from selected experimental data; Truckenbrodt (1955), Goldberg (1966), Rotta (1967), and Nash and Spalding (given by Rotta) have each proposed "universal" correlations for the first of these integrals. However, it is to be noted that these correlations differ substantially in both value and choice of correlation parameters. To employ this procedure

in the present four parameter formulation requires correlations of the dissipation integral and its first and second moments. Since correlations of the first and second moments are not available in the literature, an effort was made to determine approximate correlations of these quantities, the values of the three integrals were computed from the eddy viscosity model for all flow conditions. Figure 4 shows the correlation of these results together with the correlation equations for the first integral given by Truckenbrodt (1955) and by Escudier and Spalding (1965) for the flat plate data of Wieghardt and Tillmann (ID 1400).

Substitution of these correlation equations into the computer program in place of the numerical evaluation of the integrals indicated that the speed of computation could be increased by a factor of three but that the solutions appeared to be extremely sensitive to small errors in the correlations.

As a result of the above studies it is concluded that if adequate correlations of the dissipation integrals were available and the implicit integration scheme were employed a reduction of computer time of approximately an order of magnitude below those presented in table 1 for explicit integration could be obtained with the present method.

DISCUSSION OF RESULTS

General

The primary results presented in this paper are comparisons of predicted and experimental values of skin friction coefficient, and integral thickness parameters for sixteen different turbulent boundary layer flows. The

experimental flows considered are listed in table 1 by identification number and the name(s) of the investigator(s). More detailed results for representative flow conditions together with an assessment of the adequacy of the present method are considered below.

Experimental Data

An examination of the data studied herein suggests a division into two distinct categories. This division is based on satisfaction of the streamwise integrated, two-dimensional momentum integral equation which may be written as:

$$\int_{x_0}^x \frac{d\theta}{dx} dx + \int_{x_0}^x (z+H) \frac{\theta}{U_\infty} \frac{dU_\infty}{dx} dx = \int_{x_0}^x \frac{C_f}{z} dx \quad (11)$$

Values of θ and H (determined by integrating the experimental velocity profiles) and C_f (determined by matching experimental velocity profiles and law of the wall profiles) obtained at successive survey stations may be introduced into (11), along with the experimental values of U_∞ and dU_∞/dx , and integrated from x_0 to any downstream station x . Just such an analysis was carried out by Kline et al (1968) for all of the sets of data studied herein. It was found that for some flows, the left and right hand sides of equation (11) diverged at some streamwise station. Based on the above discussion, the data were divided into the two categories presented in table 2. The first category contains all of those flows, or portions of flows, which reasonably satisfy equation (11) and the second category contains those flows, or portions of flows, which do not satisfy equation (11). A detailed discussion of flows in the second category will not be given since any flows satisfying equations (1) and (2) must necessarily satisfy (11). However, comparisons of those data with

the present method will be presented for completeness.

Comparison of Predicted and Experimental Results

The comparisons of predicted and experimental values of H , C_f and Re_θ are given in the figures showing the collected comparisons. For those flows satisfying the momentum integral balance, the predictions of H , C_f , and Re_θ are in good agreement with the data except for the flows with a large wake component.

Figure 5 shows a comparison of experimental and predicted velocity profiles at four stations of the Schubauer and Klebanoff flow (ID 2100). As can be seen, good agreement between experiment and prediction is obtained everywhere except at the 22 foot station where the boundary layer has been subjected to an adverse pressure gradient over the preceding five feet.

Similar agreement at the initial stations and subsequent degradation of accuracy is shown in figures 6, 7, and 8 for the flows of Ludwig and Tillmann (ID 1100), Clauser (ID 2200), and Clauser (ID 2300), respectively. This lack of agreement gave rise to an investigation into the character of the velocity profiles which could be described by the currently employed velocity gradient profile, γ .

In an effort to determine the flexibility of the presently employed profile, a flow representative of those having large wake components, i.e., Clauser (ID 2300) was examined. The velocity profile at the initial station was replotted on law of the wall coordinates in figure 9. It was found that the representation of the initial profile could be forced to agree with the data in the wake region, figure 9a, or in the wall region figure 9b, but not

in both regions. Therefore, it is concluded that the ^{four parameter} ~~polynomial~~ representation of the velocity profile is inadequate to represent velocity profiles with large wake components.

In contrast to the above, flows with moderate wake components, e.g. Clauser (ID 2200), can be described reasonably well with the present formulation. This conclusion is substantiated by the results presented in figure 10.

For those flows where the momentum integral balance is not satisfied, large wake components are usually present. This clouds the comparisons of predictions with data, since at the outset, equations (1) and (2) are invalid.

CONCLUSIONS

The intent of the present study was to determine the efficiency and accuracy of a generalized moment method in the solution of the incompressible turbulent boundary layer equations. Relatively large computing times were required to obtain solutions for the flows considered. This was the result of the time consuming numerical evaluation of the dissipation integral and its two additional moments. By using an accurate correlation of these integrals the quoted run times can be reduced by approximately 70%. The accuracy of the present formulation of the generalized moment method is acceptable for flows without large wake components. For flows with large wake components, the accuracy may be improved by employing more physically realistic velocity gradient profiles.

It is believed that despite certain shortcomings of the present formulation, the moment method provides a powerful tool in the solution of partial differential equations. In addition, with a modification of the velocity profile to account for the presence of large wakes and the reduction in

computing time which has been shown to be possible, the method should prove useful both in turbulent boundary layer research and as a design tool.

Extension of moment methods, in particular, and any computing scheme, in general, to separating flows will require a substantially better understanding of the physical processes involved.

REFERENCES

- BETHEL, H.E. and ABBOTT, D.E.: On the convergence and exactness of solutions of the laminar boundary layer equations using the N parameter integral formulation of Galerkin-Kantorovich-Dorodnitsyn. School of Mech. Eng., Tech Rpt FMTR 66-2, Purdue University, April 1966.
- DEIWERT, G.S. and ABBOTT, D.E.: On the analysis of the turbulent boundary layer by the method of weighted residuals. School of Mech. Eng., Tech Rpt FMTR 67-2, Purdue Univ., Nov. 1967.
- DORODNITSYN, A.A.: General method of integral relations and its application to boundary layer theory. Advances in Aeronautical Sciences, vol. III, Macmillan, New York, 1960, pp 207-219.
- ESCUDIER, M.P. and SPALDING, D.B.: A note on the turbulent uniform property hydrodynamic boundary layer on a smooth impermeable wall: Comparisons of theory with experiment. ME Dept., Imperial College, London, 1965.
- GOLDBERG, P.: Upstream history and apparent stress in turbulent boundary layers. MIT Gas Turbine Lab Rpt No. 85, May 1966.
- HOLT, M.: Separation of laminar boundary layers on cooled re-entry bodies. IAF-IAC, 18th Congress, Madrid, A-67-12348, Oct. 9-10, 1966
- KANTOROVICH, L.V., and KRYLOV, V I.: Approximate methods of higher analysis. Interscience, New York, 1964.
- KENDALL, Robert M. and BARTLETT, Eugene P.: Non-similar solutions of the multi-component laminar boundary layer by an integral matrix method. AIAA preprint 67-218, Presented at the 5th Aerospace Sciences Meeting, New York, Jan. 23-26, 1967.
- LOMAX, Harvard: An operational unification of finite difference methods for the numerical integration of ordinary differential equations. NASA TR-262, 1967.
- LOMAX, H. and BAILEY, H.E.: A critical analysis of various numerical integration methods for computing the flow of a gas in chemical nonequilibrium. NASA TN D-4109, Aug. 1967.
- MIKHLIN, G. and SMOLITSKIY, K.L.: Approximate methods for solution of differential and integral equations. Trans. Ed. Robt. E. Kalaba, American Elsevier Publishing Co., New York, 1967.
- MOSES, Hal L.: The behavior of turbulent boundary layers in adverse pressure gradients. MIT Gas Turbine Lab, Rpt No. 73, Jan. 1964.
- NIELSEN, J.N., LYNES, L.L., and GOODWIN, F.K.: Calculation of laminar separation with free interaction by the method of integral relations. Part II - Two dimensional supersonic non-adiabatic flows and axisymmetric supersonic adiabatic and non-adiabatic flows. AFFDL TR 65-107, Part II - Jan. 66

- PALLONE, Adrian: Nonsimilar solutions of the compressible-laminar boundary-layer equations with applications to the upstream-transpiration cooling problem. Journ. Aero/Space Sci., vol. 28 No. 6, pp 449-456 and 492, June 1961.
- PAVLOVSKII, Y.N.: The numerical calculation of the laminar boundary layer in a compressible gas. USSR Computational Mathematics and Mathematical Physics, No. 5, 1963, Pergamon Press, Aug. 1964.
- PETRYSHYN, W.V.: Projection methods in nonlinear numerical functional analysis. Journal of Mathematics and Mechanics, vol. 17, pp 353-372.
- ROTTA, J.C.: Critical review of existing methods for calculating the development of turbulent boundary layers. Paper presented at Symposium on the Fluid Mechanics of Internal Flow, Warren, Mich. 1965, Elsevier, Pub. Co., New York, 1967, Gino Sovran Ed.
- SMITH, A.M.O., JAFFE, N.A. and LIND, R.C.: Study of a general method of solution to the incompressible turbulent boundary layer equations. Douglas Acft. Div., Rpt No. L.B. 52949, 11 Nov. 1965.
- TRUCKENBRODT, E.: A method of quadrature for calculation of the laminar and turbulent boundary layer in case of plane and rotationally symmetrical flow., NACA TM 1379, May 1955, translated from Ing Archiv Band XX, Viertes Heft (1952).

TABLE I

ID NUMBER	INVESTIGATOR	RUN TIMES (7094 MIN.)	
		<u>Explicit</u>	<u>Implicit</u>
1100	Ludwig and Tillmann	4.77	
1200	Ludwig and Tillmann	2.96	
1300	Ludwig and Tillmann	5.08	
1400	Wieghardt and Tillmann	4.87	1.85
1500	Tillmann	10 ⁺	2.95
2100-I ¹	Schubauer and Klebanoff	10.97	4.95
2100-II ²	Schubauer and Klebanoff	2.00	
2200	Clauser	3.61	
2300	Clauser	5.94	
2400	Bradshaw	4.38	
2500	Bradshaw	1.61	
2600	Bradshaw	7.09	
2700-I ³	Herring and Norbury	2.01	
2700-II ⁴	Herring and Norbury	2.19	
2900	Perry	8.00	3.70
3500	Newman	2.71	
3800	Moses	1.22	
4000	Moses	10 ⁺	4.00

1. $x_0 = 1.5$ feet

2. $x_0 = 19$ feet

3. Investigators first pressure distribution.

4. Investigators second pressure distribution.

TABL 2

CATEGORY I
 FLOWS SATISFYING MOMENTUM
 INTEGRAL BALANCE

<u>ID</u>	<u>INVESTIGATOR</u>	
1100	Ludwig & Tillmann	x < 3 meters
1200	Ludwig & Tillmann	x < 3 meters
1300	Ludwig & Tillmann	All x considered
1400	Wieghardt & Tillmann	All x considered
2100	Schubauer & Klebanoff	x < 22 feet
2200	Cluser	All x considered
2300	Cluser	All x considered
2500	Bradshaw	All x considered
2600	Bradshaw	All x considered
2700	Herring & Norbury	All x considered
3500	Newman	All x considered
3800	Moses	x < 1.2 feet
4000	Moses	x < 0.5 feet

CATEGORY II
 FLOWS NOT SATISFYING MOMENTUM
 INTEGRAL BALANCE

<u>ID</u>	<u>INVESTIGATOR</u>	
1100	Ludwig & Tillmann	x > 3.0 meters
1200	Ludwig & Tillmann	x > 3.0 meters
1500	Tillmann	All x considered
2100	Schubauer & Klebanoff	x > 22 feet
2400	Bradshaw	All x considered
2900	Perry	All x considered
3800	Moses	x > 1.2 feet
4000	Moses	x > 0.5 feet

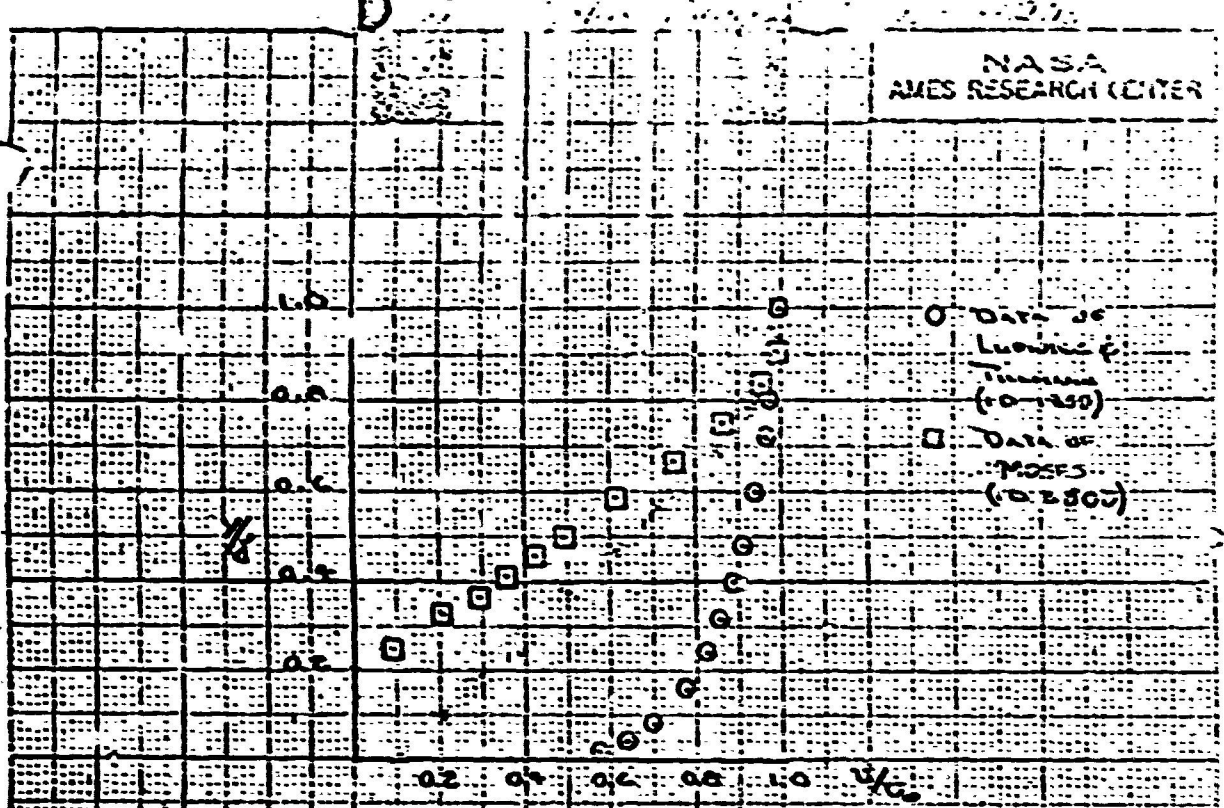


FIG. 1 APPROXIMATE RANGE OF VELOCITY PROFILES CONSIDERED

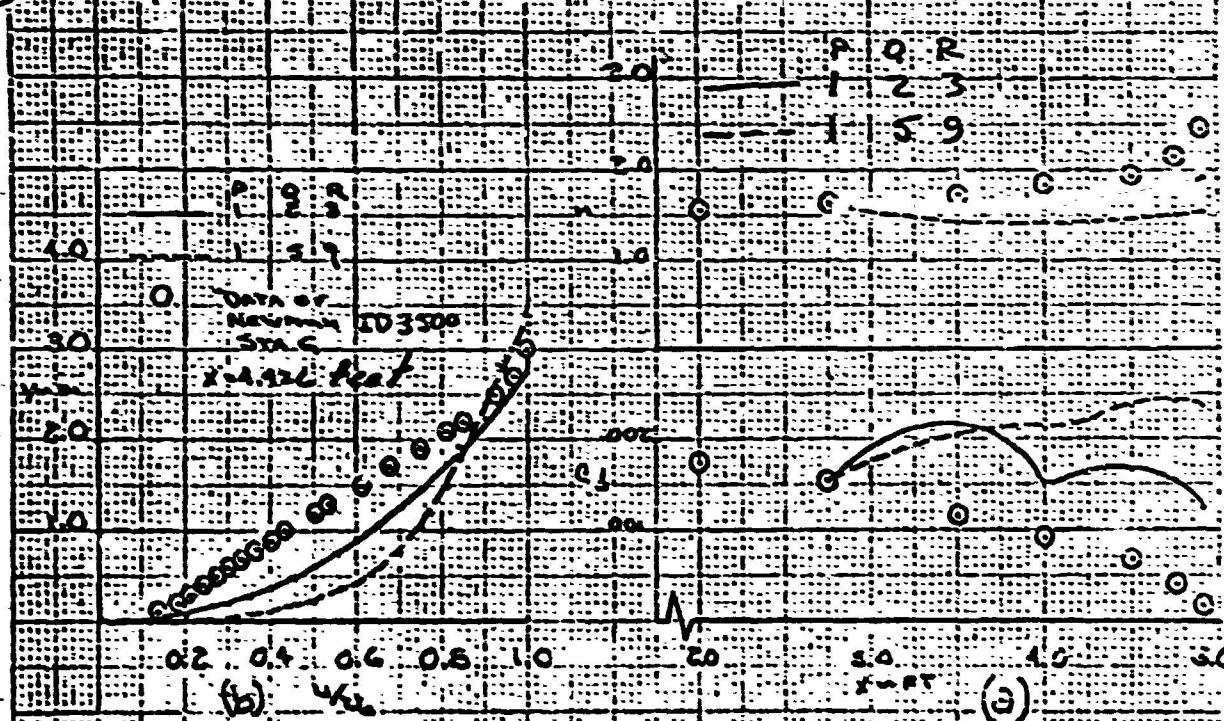


FIG. 2 EFFECTS OF THE CHOICE OF VELOCITY GRADIENT PROFILE EXPONENTS ON FLOW PARAMETERS FOR SEVERE ADVERSE PRESSURE GRADIENT FLOW

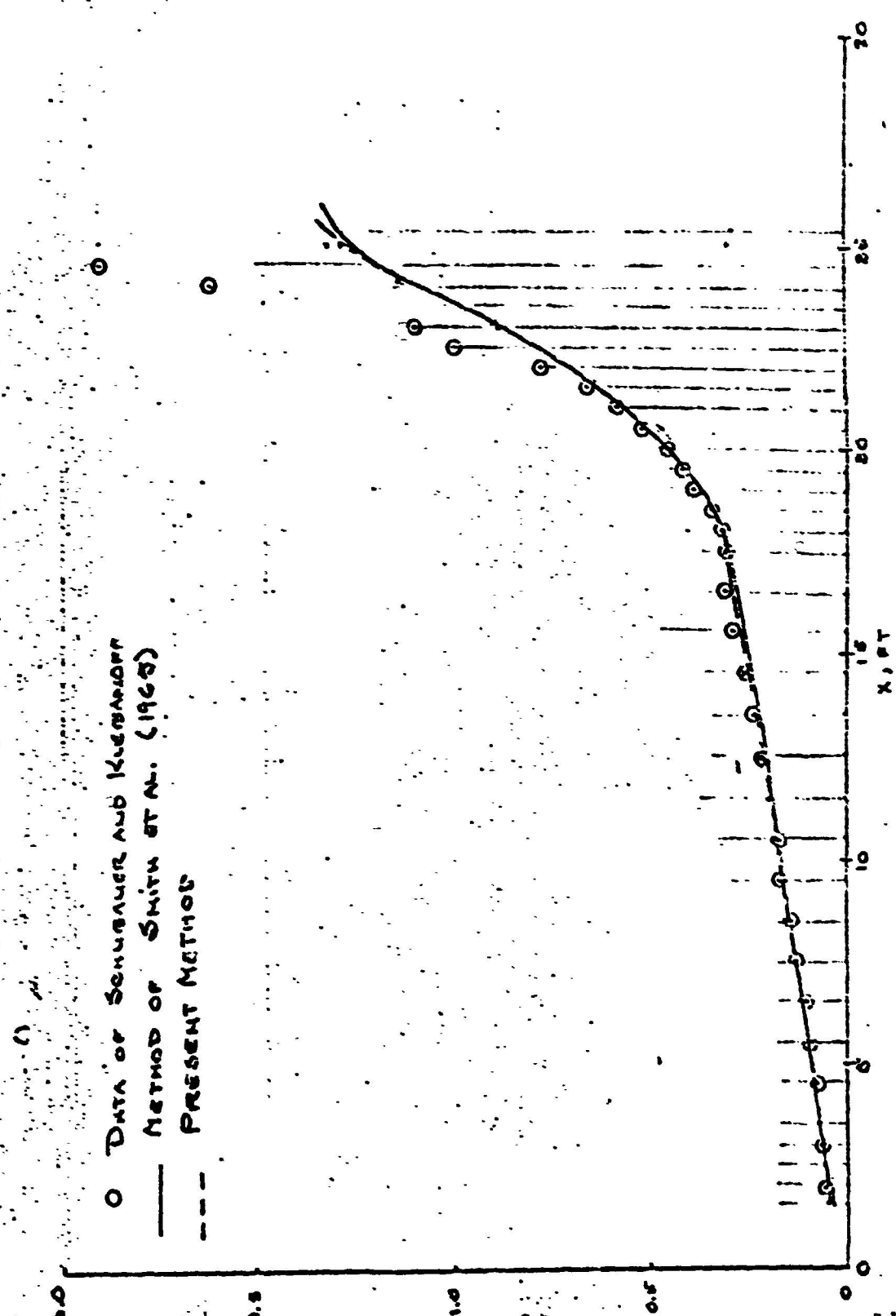


FIGURE 3. COMPARISON OF THE RESULTS OF THE PRESENT METHOD WITH
 THE EXACT NUMERICAL SOLUTION OF SMITH ET AL. (1968) FOR
 THE FLOW OF SCHUBAUER AND KLEBANOFF (ID 2100).

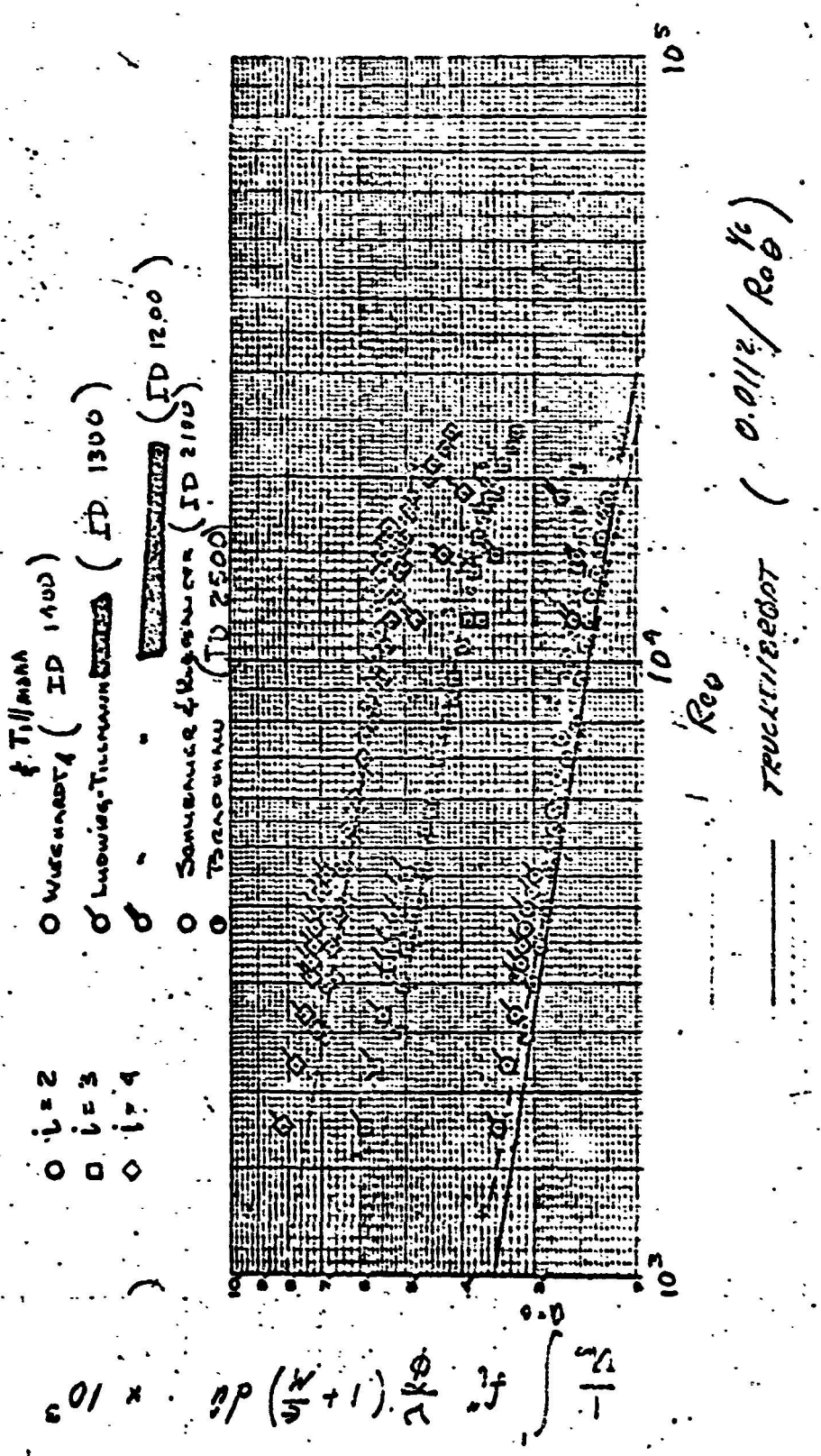
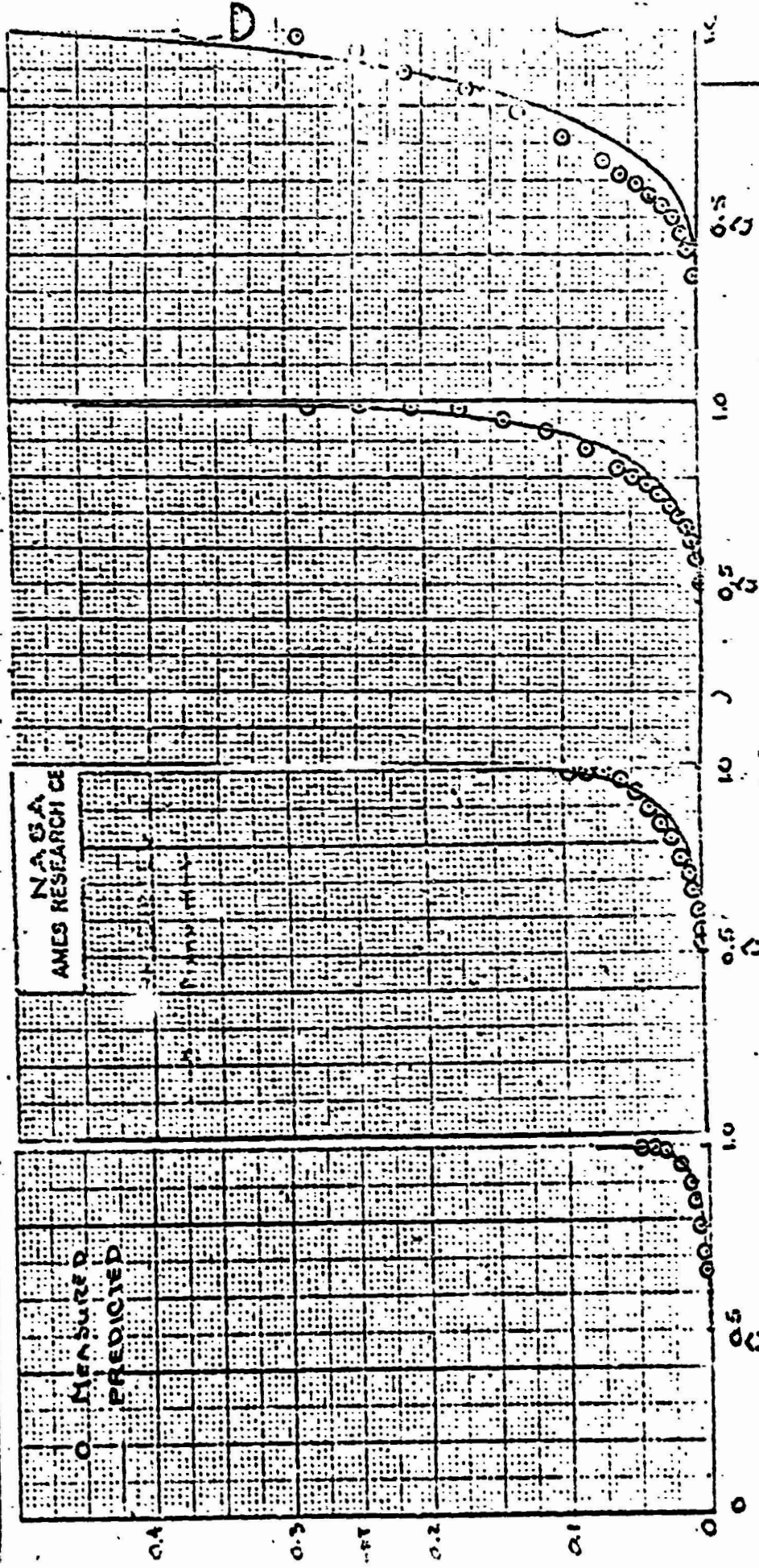
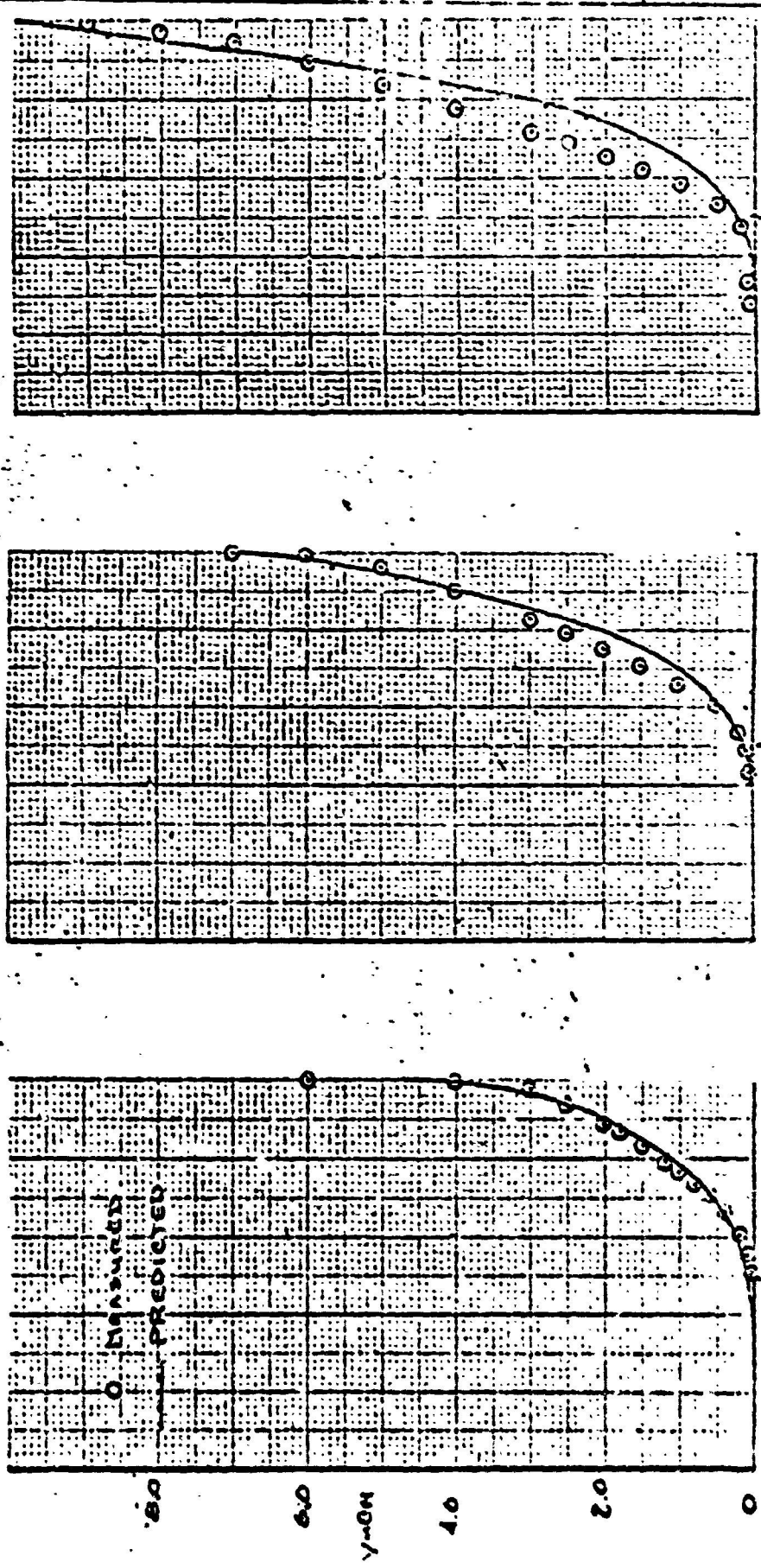


Figure A. Correlation of Spire Antiquated Dredged from study locality 1830.



a) X = 1.5 FEET b) X = 7.5 FEET c) X = 17.5 FEET d) X = 22.0 FEET
FIGURE 25 COMPARISON OF EXPERIMENTAL AND PREDICTED VELOCITY PROFILES
DATA OF GUMMINGER AND KLEBANOFF ID 2100



a) $x = 1.252$ METERS b) $x = 2.582$ METERS c) $x = 3.152$ METERS

FIGURE 6. COMPARISON OF EXPERIMENTAL AND PREDICTED VELOCITY PROFILES
DATA OF LARQUIER AND TULLIANNI (20 1100)

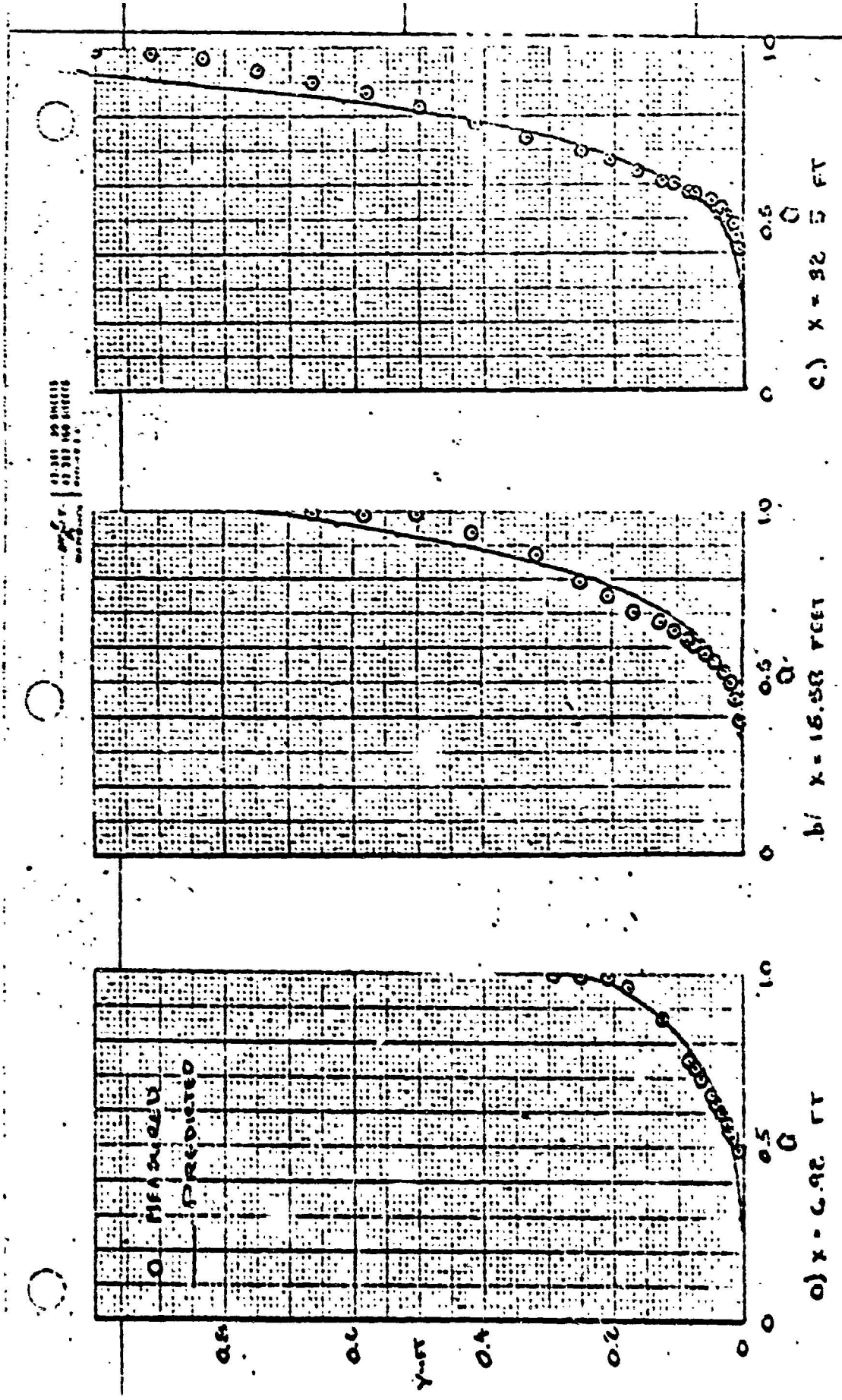
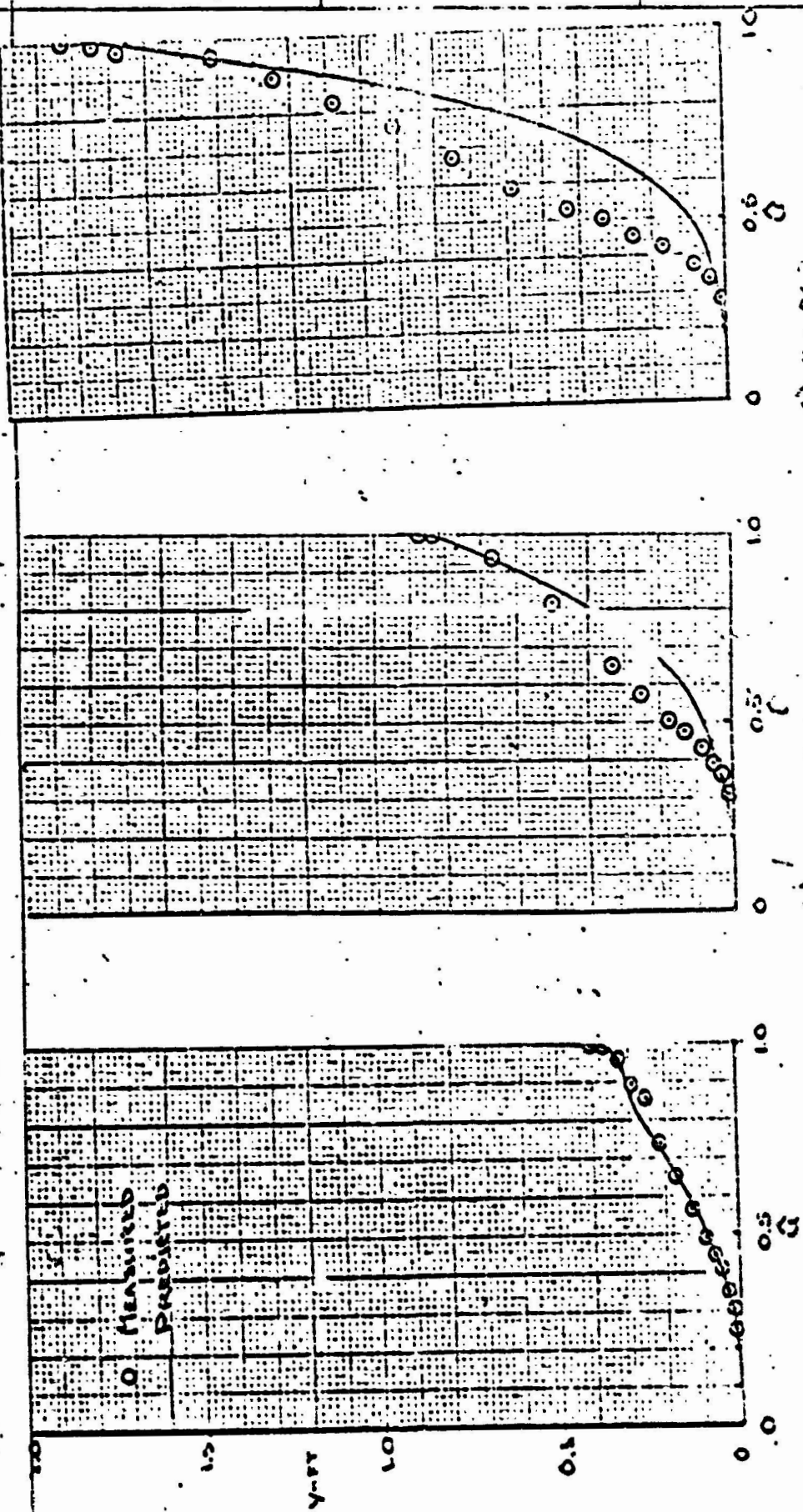
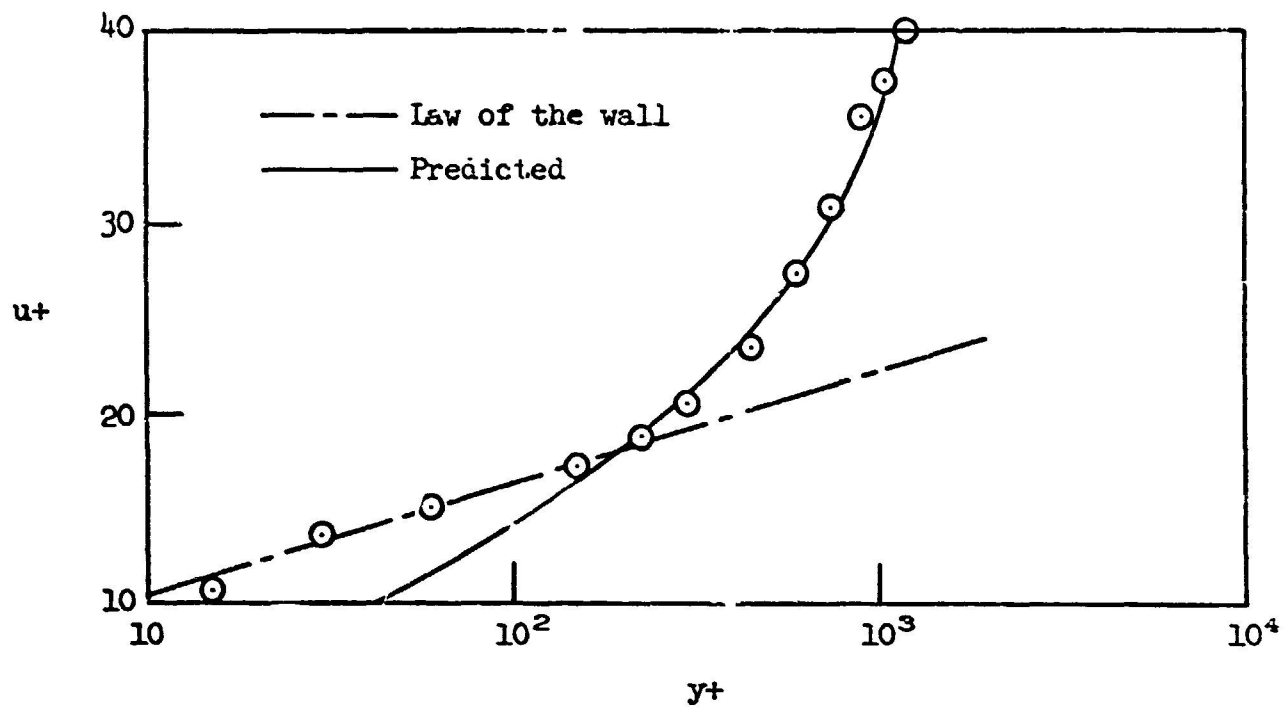


FIGURE 7 COMPARISON OF EXPERIMENTAL AND PREDICTED VELOCITY PROFILES
 DATA OF CLINCK (PRESSURE DISTRIBUTION) 10 2200

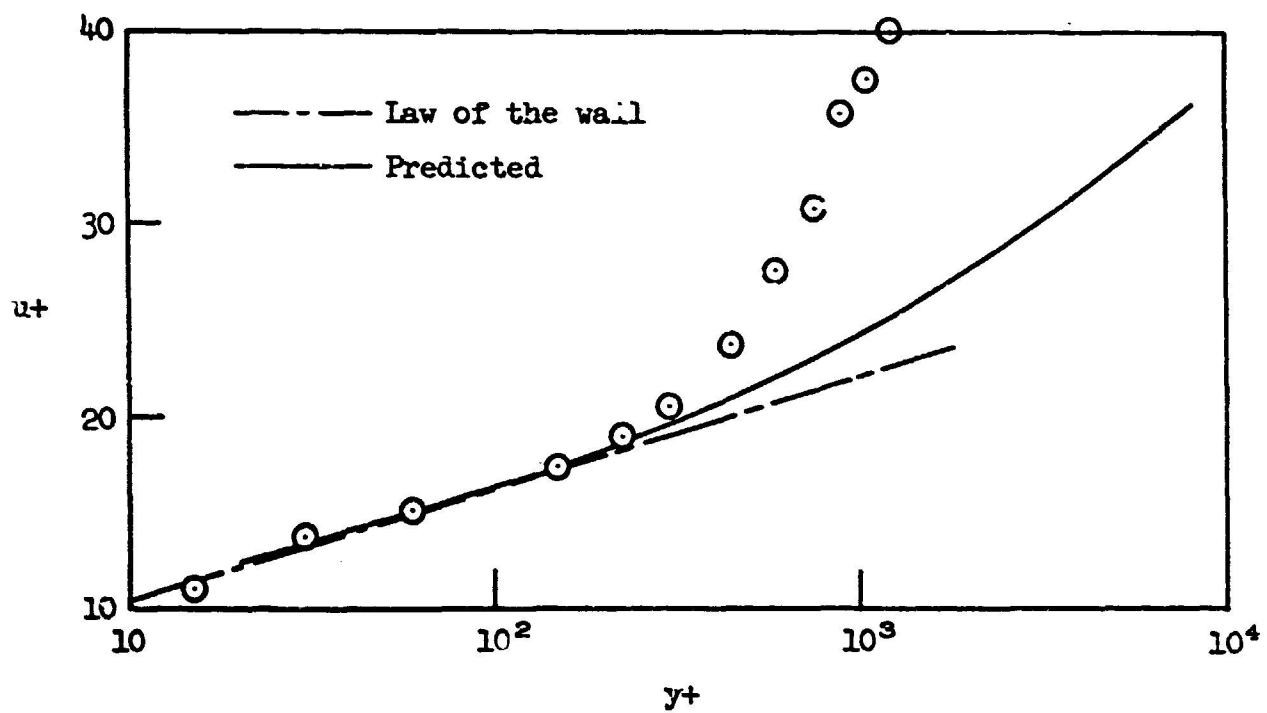


a) $x = 9.0$ FEET
 b) $x = 16.2$
 c) $x = 24.7$

FIGURE 8
 COMPARISON OF EXPERIMENTAL AND PREDICTED VELOCITY PROFILES
 DATA OF CLAUSER (PRESSURE DISTRIBUTION #2) IN 2500



(a) Matching velocity profile in wake region



(b) Matching velocity profile in wall region

Figure 9.- Comparison of initial velocity profiles for the present method with experimental data from a flow having a large wake component data of Clauser (ID 2300), $x = 9.0$ feet.

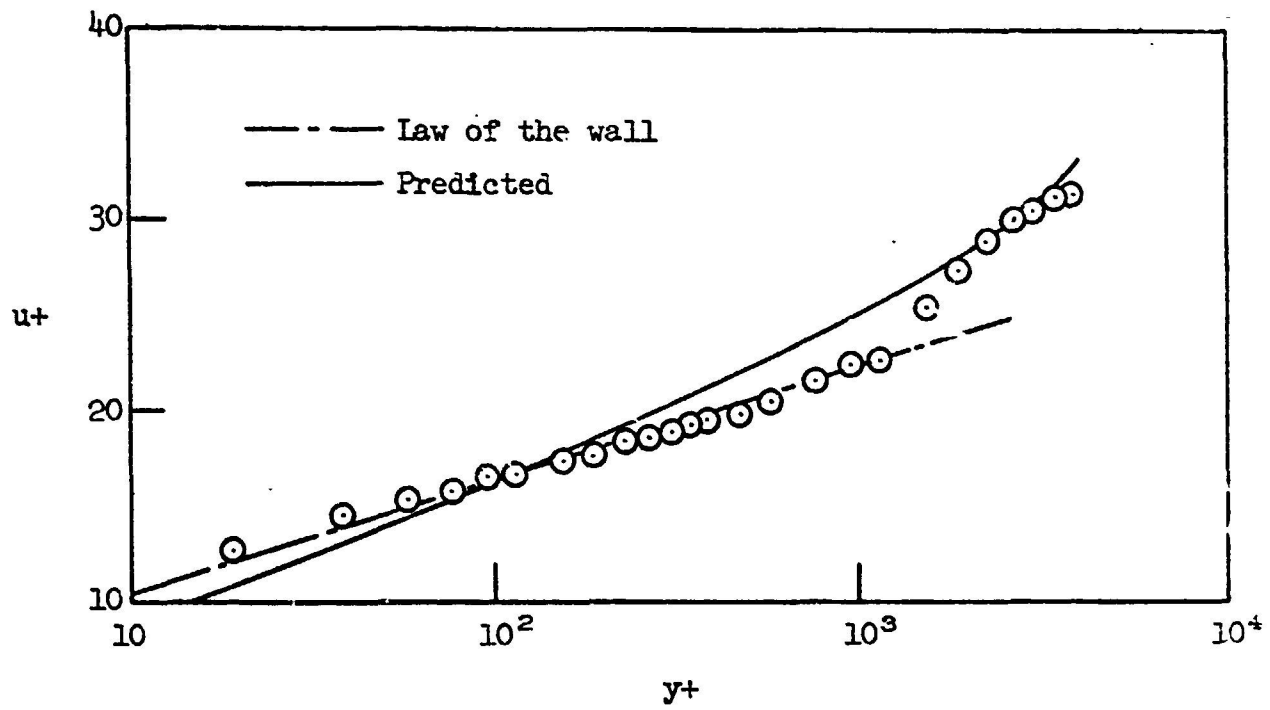
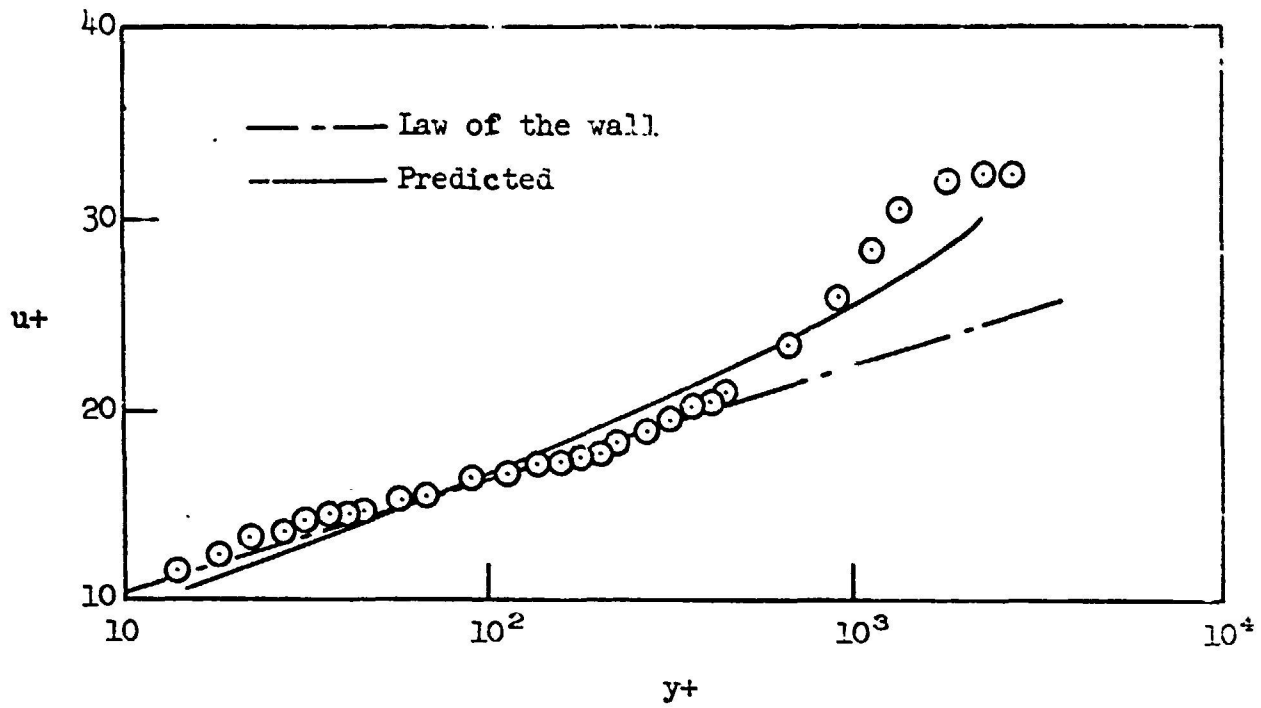
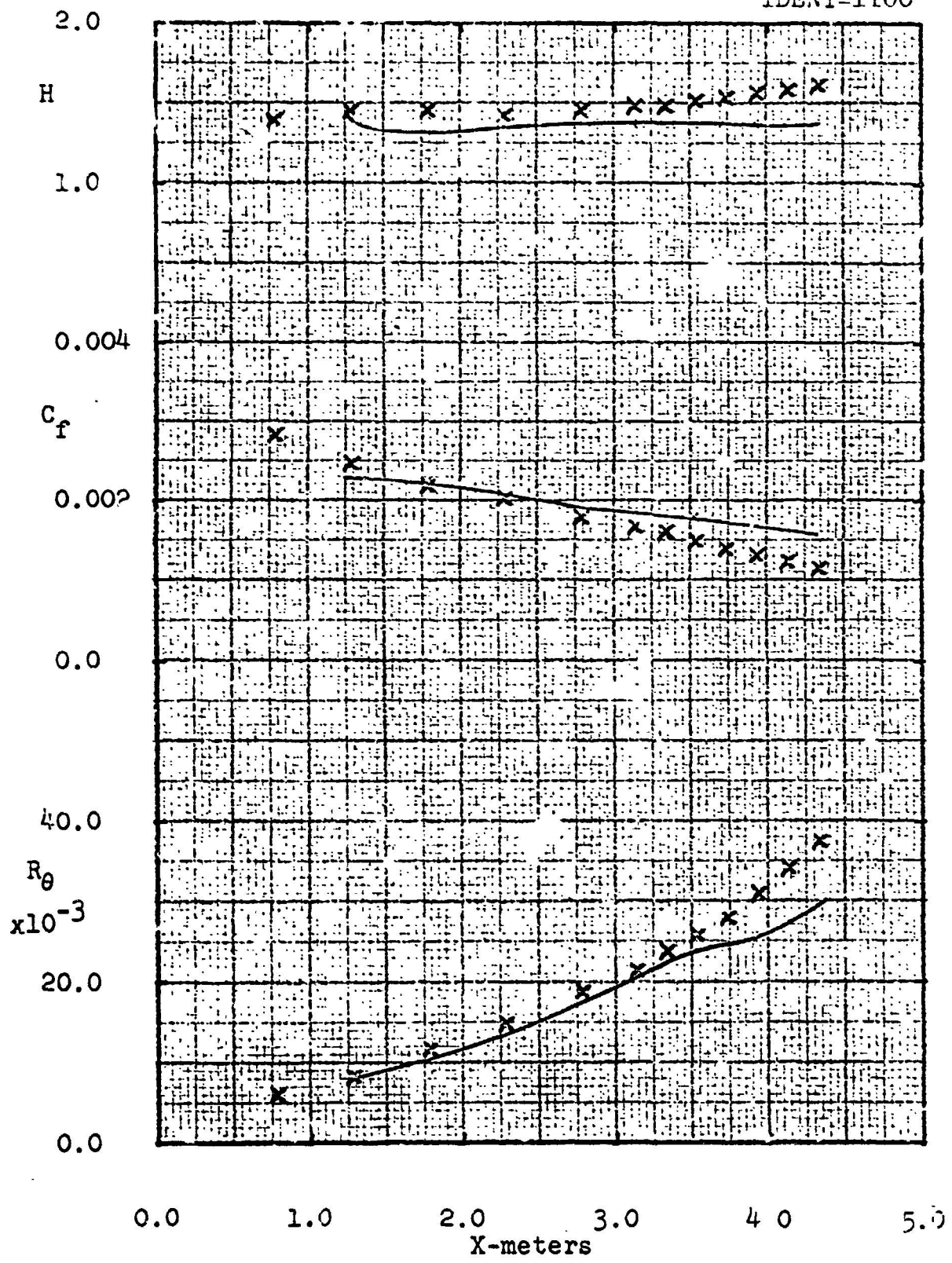


Figure 10.- Comparison of present method with flow with a moderate wake component data of Clauser (ID 2200).

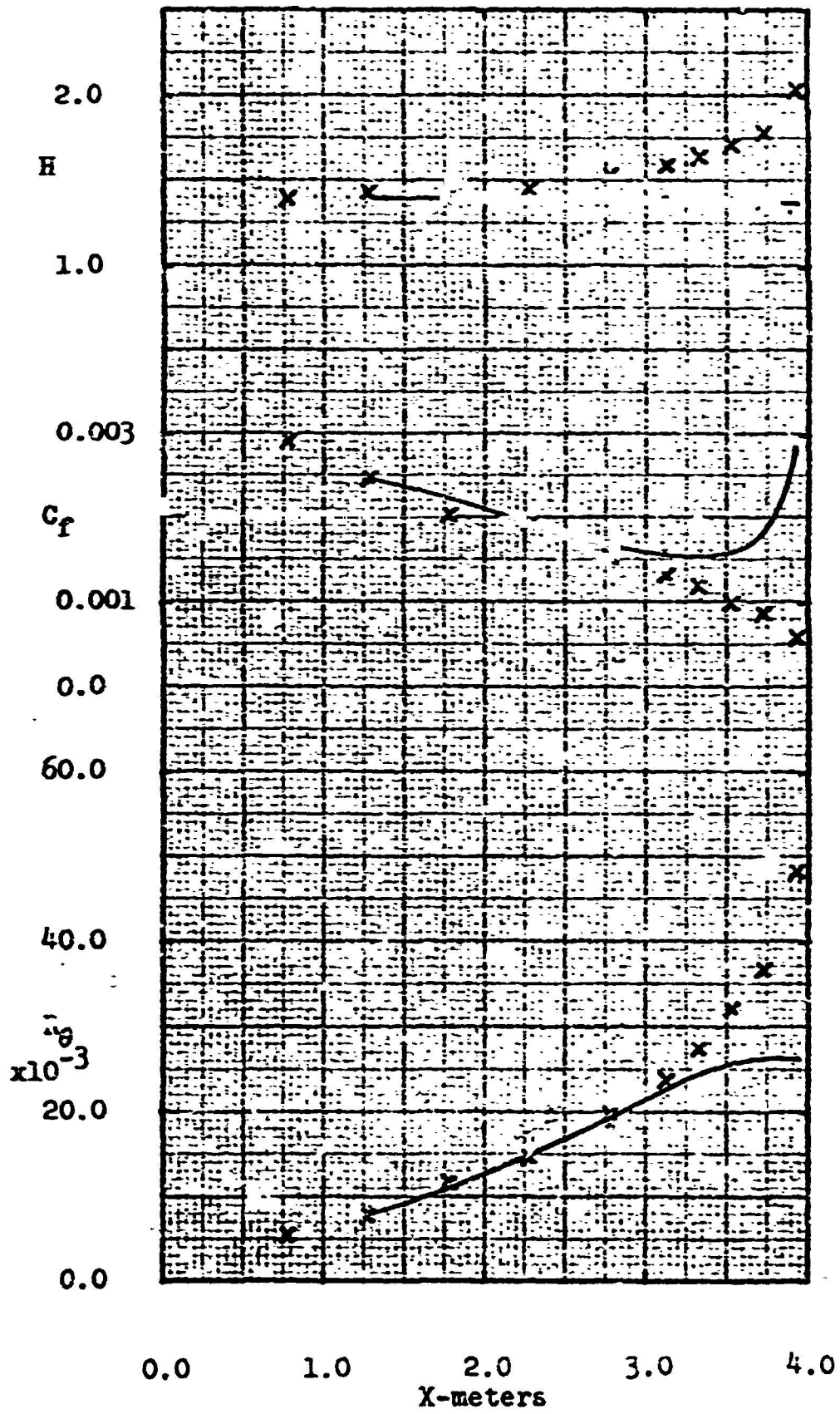
LUDWIG AND TILLMANN
MILD ADVERSE PRESSURE GRADIENT

IDENT=1100



LUDWIG AND TILLMANN
STRONG ADVERSE PRESSURE GRADIENT

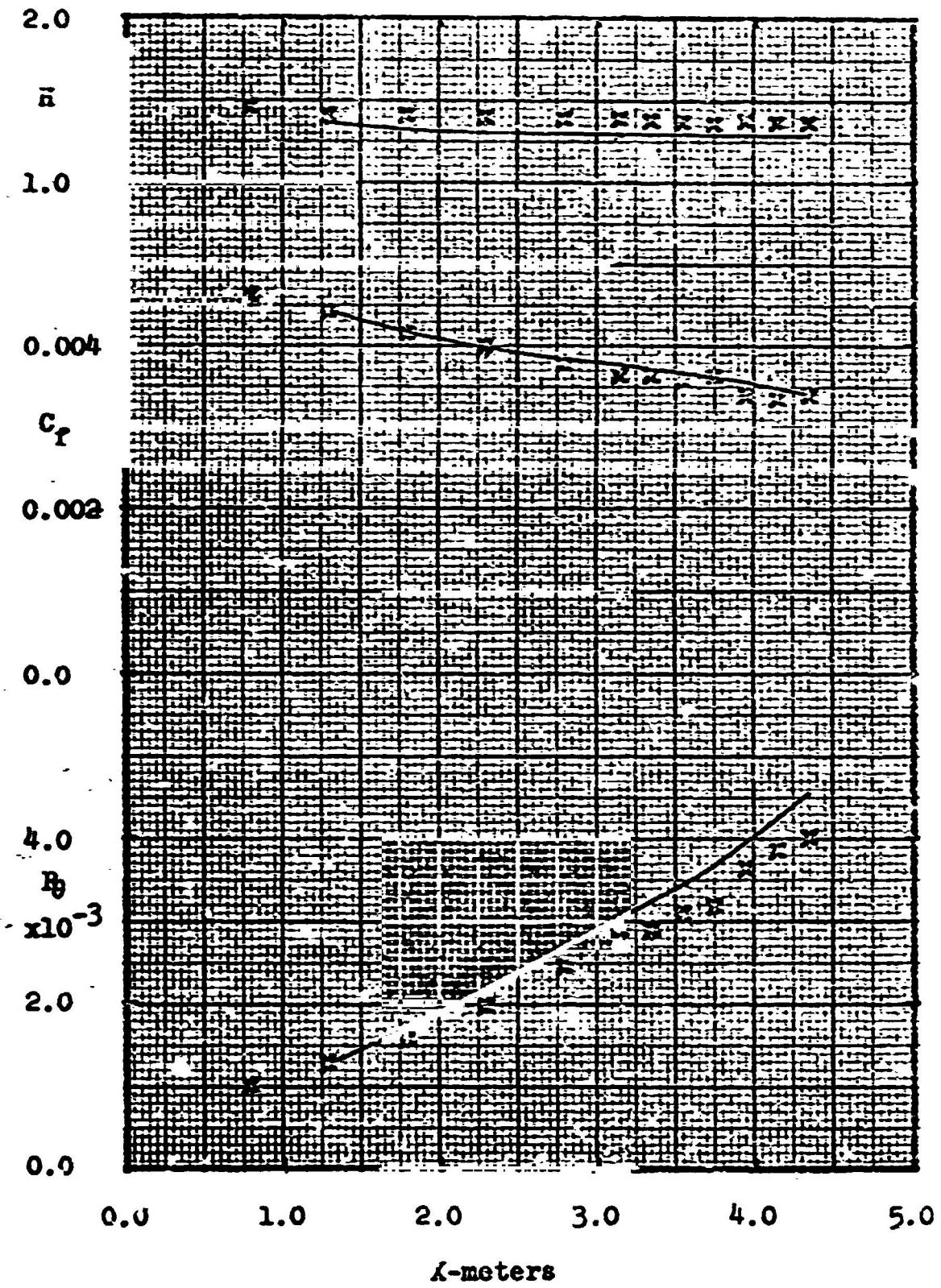
ReNT=1200



MUDWIEG AND TILLMANN

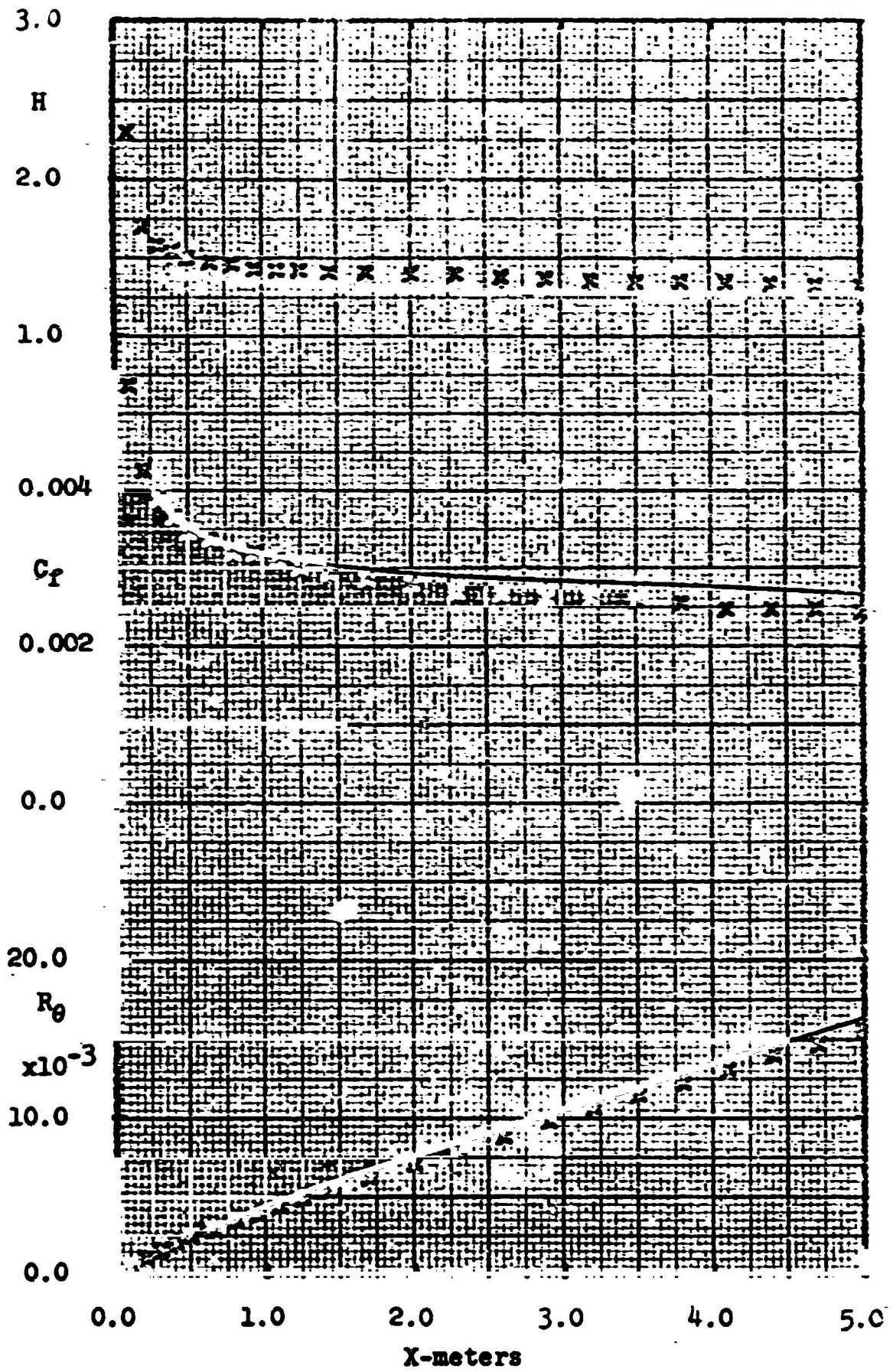
ACCELERATING FLOW

IDENT=1300



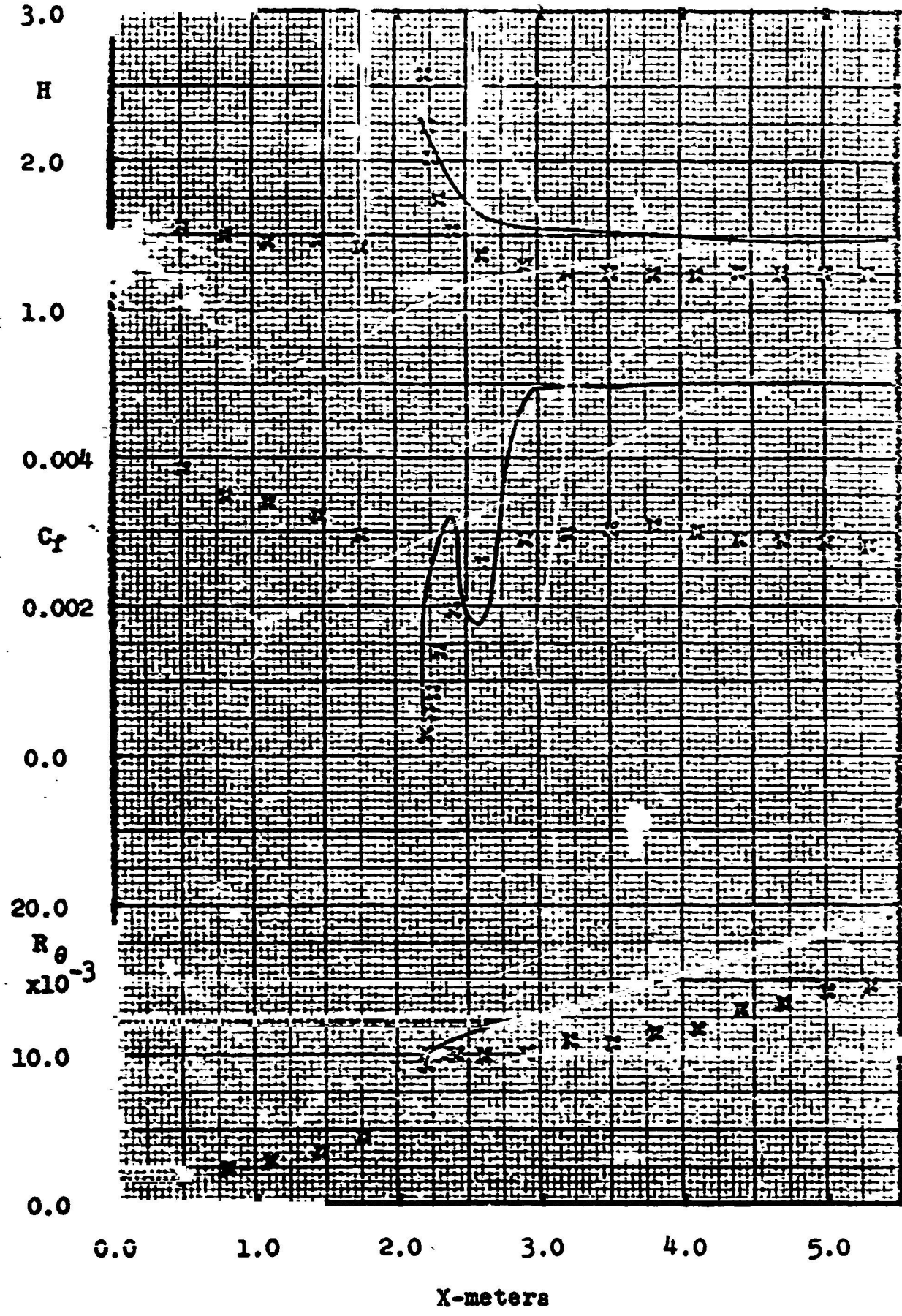
WINDHARDT FLAT PLATE FLOW

IDENT-1400



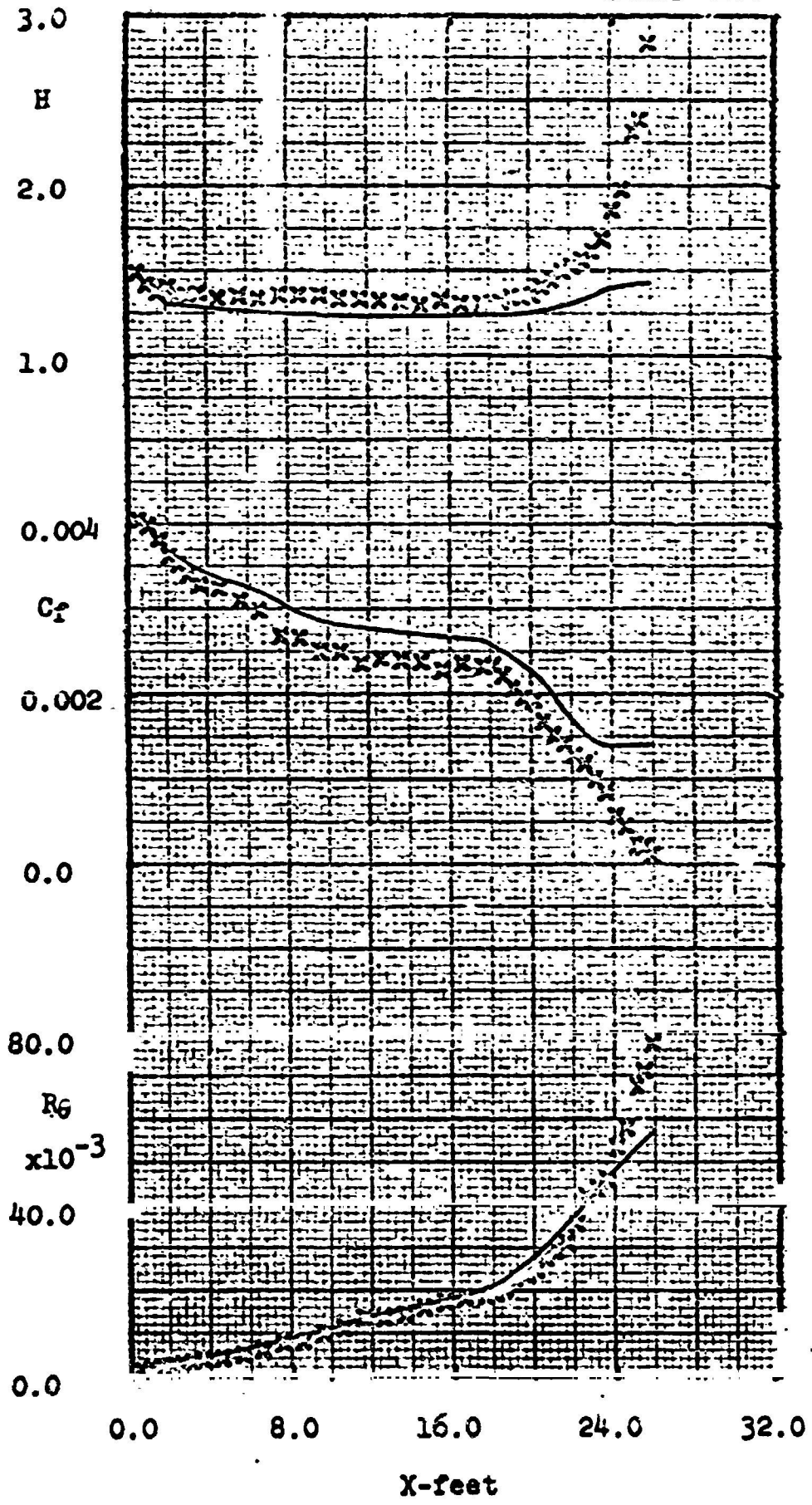
MILLMANN LEDGE FLOW

IDENT=1500



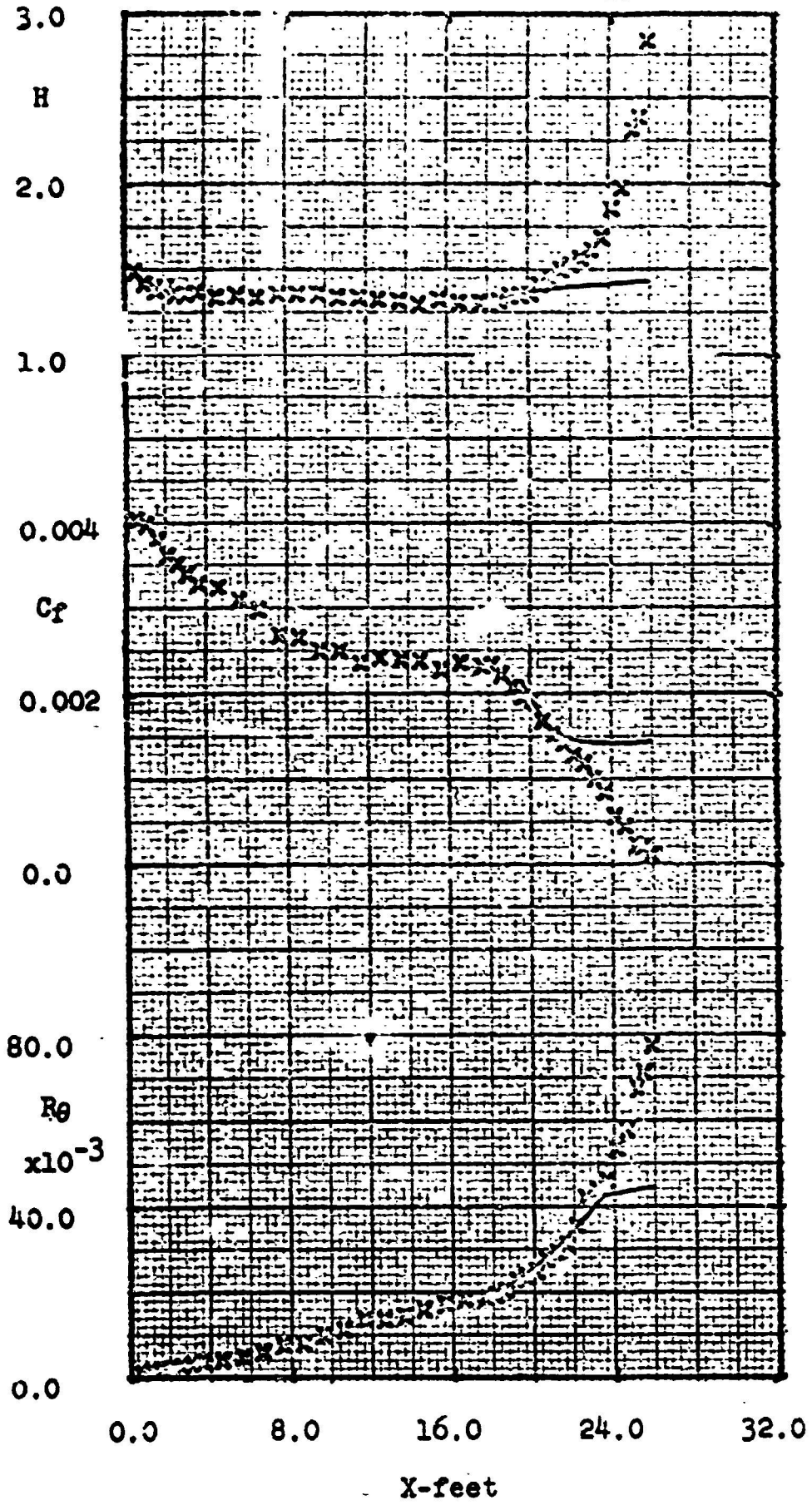
BUCHBAUER AND KLEBANOFF

IDENT=0100



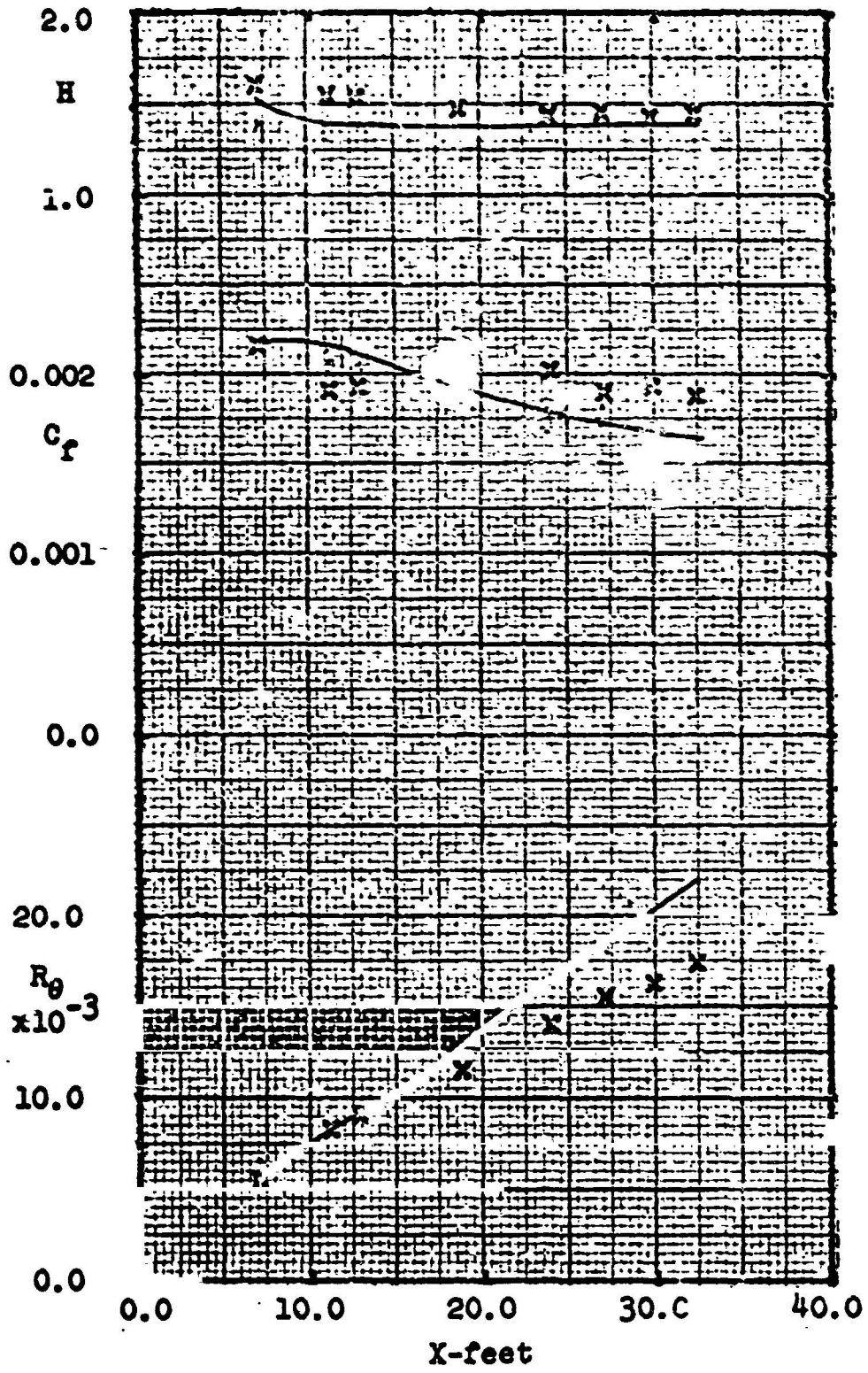
HUBAUM AND KLEBANOFF

IDENT-2100



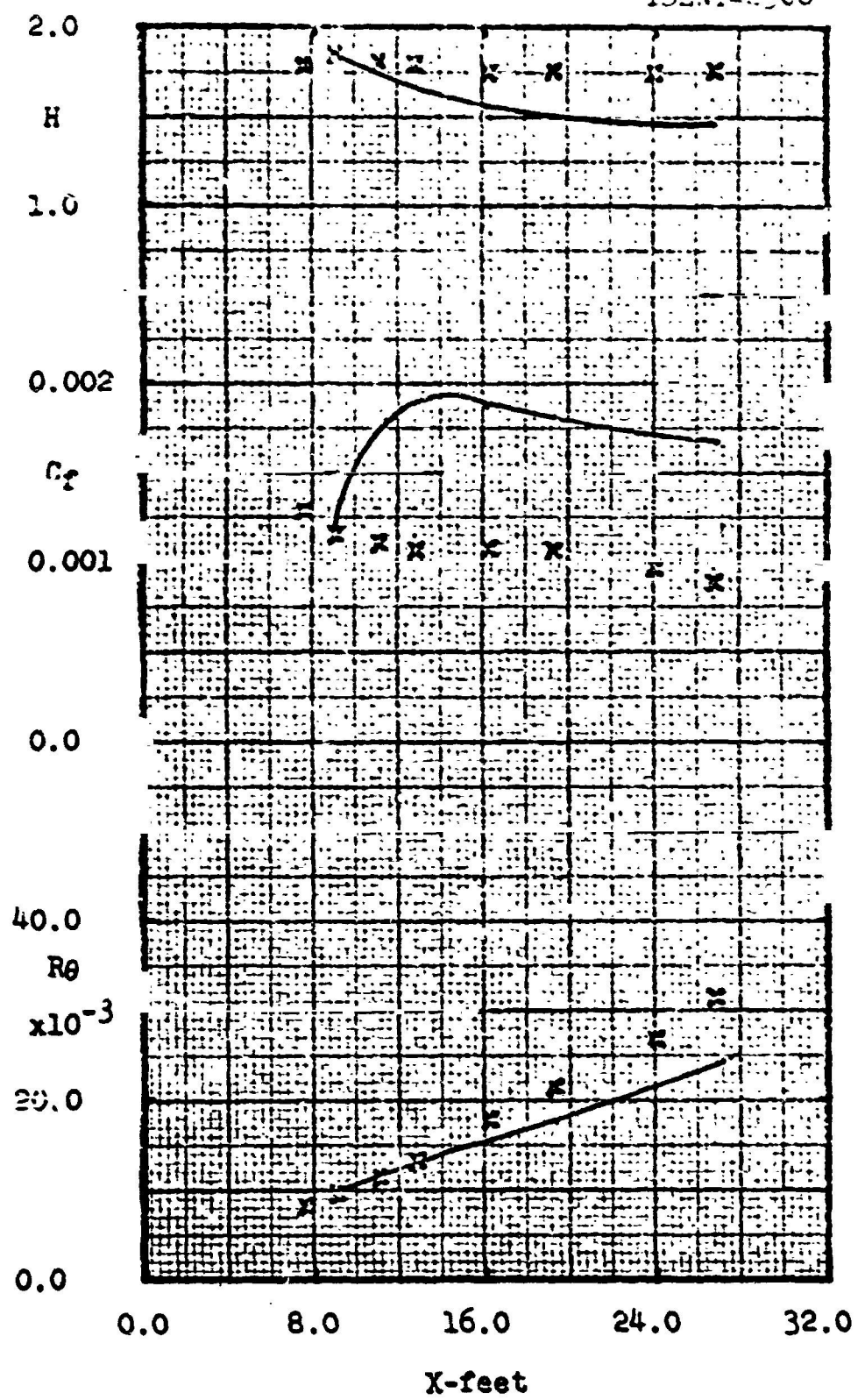
CLAUSEN NUMBER 1

IDENT = 2200



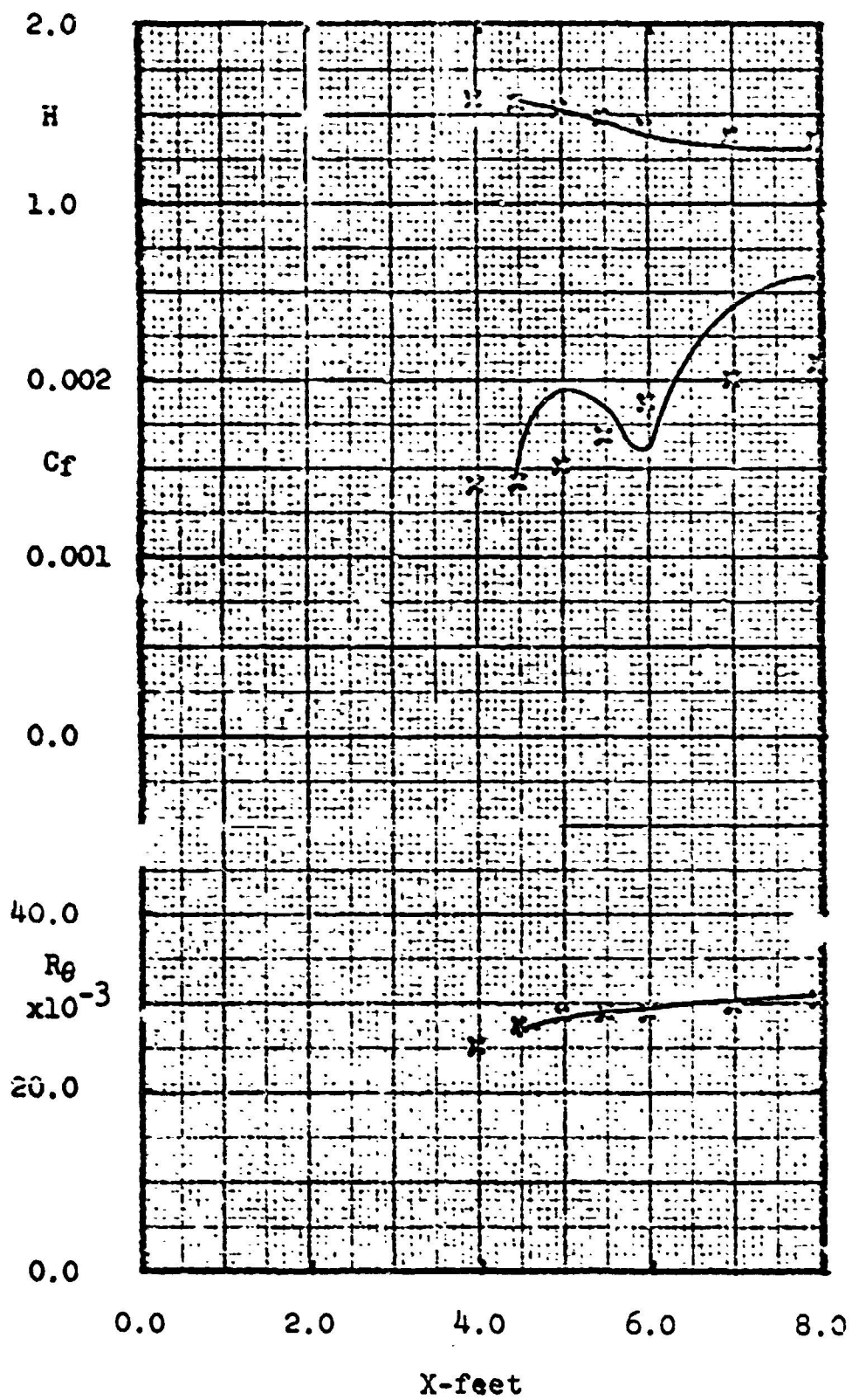
CLAUSER NUMBER 2

IDENT-2300



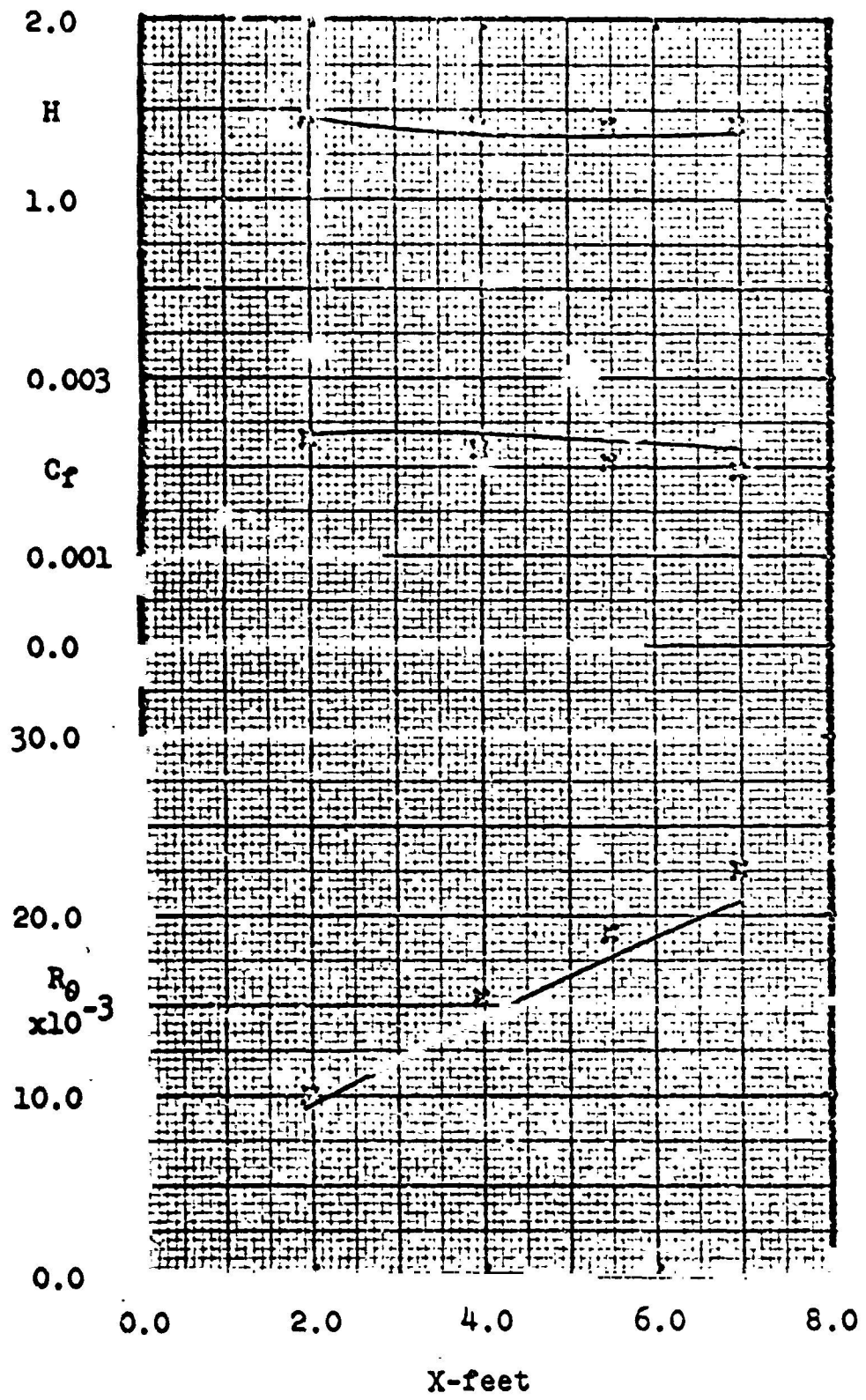
BI ADSHAW RELAXING FLOW

IDENT=2400



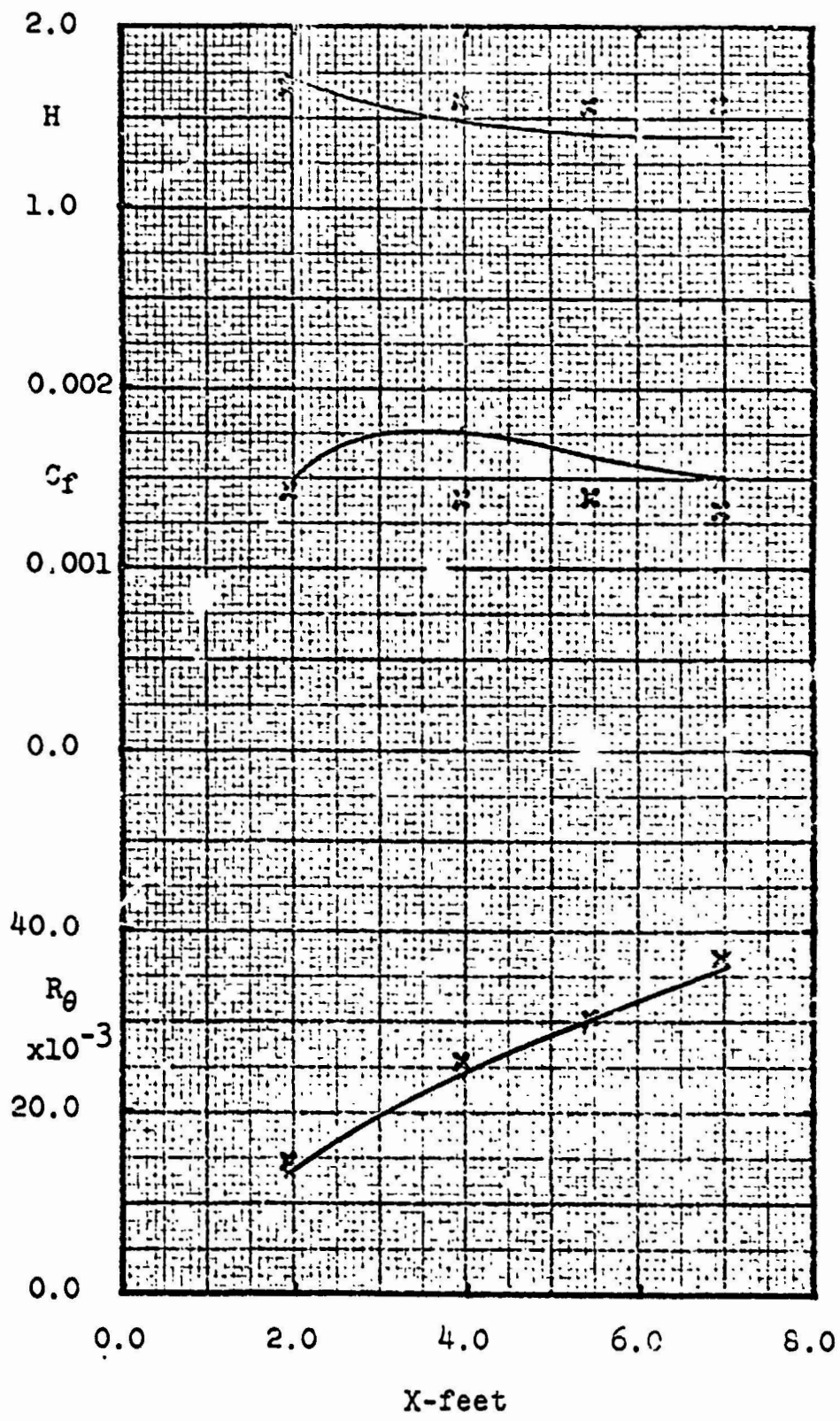
BRADSHAW $a=-0.15$

IDENT=2500



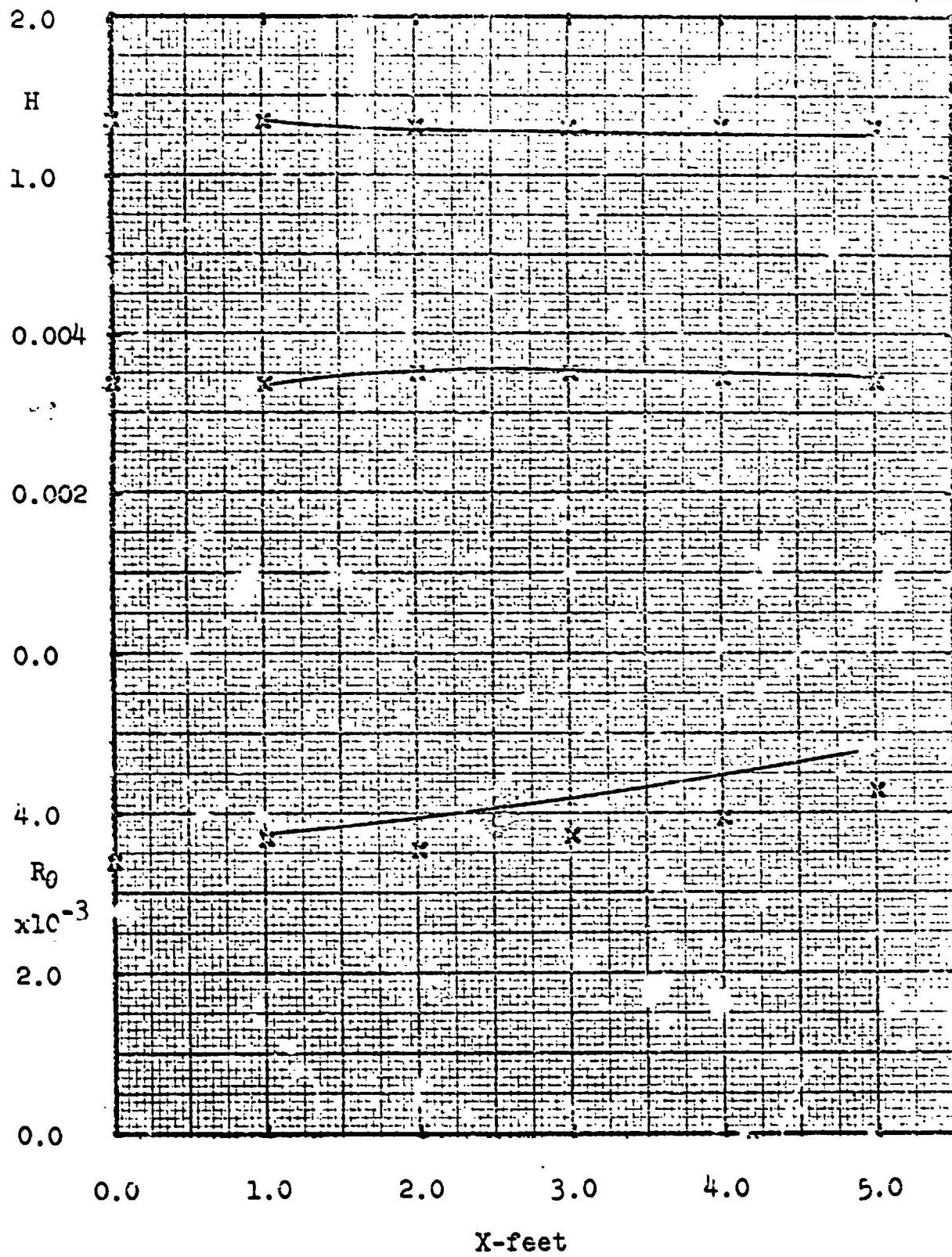
BRADSHAW $\alpha = -0.255$

IDENT=2600



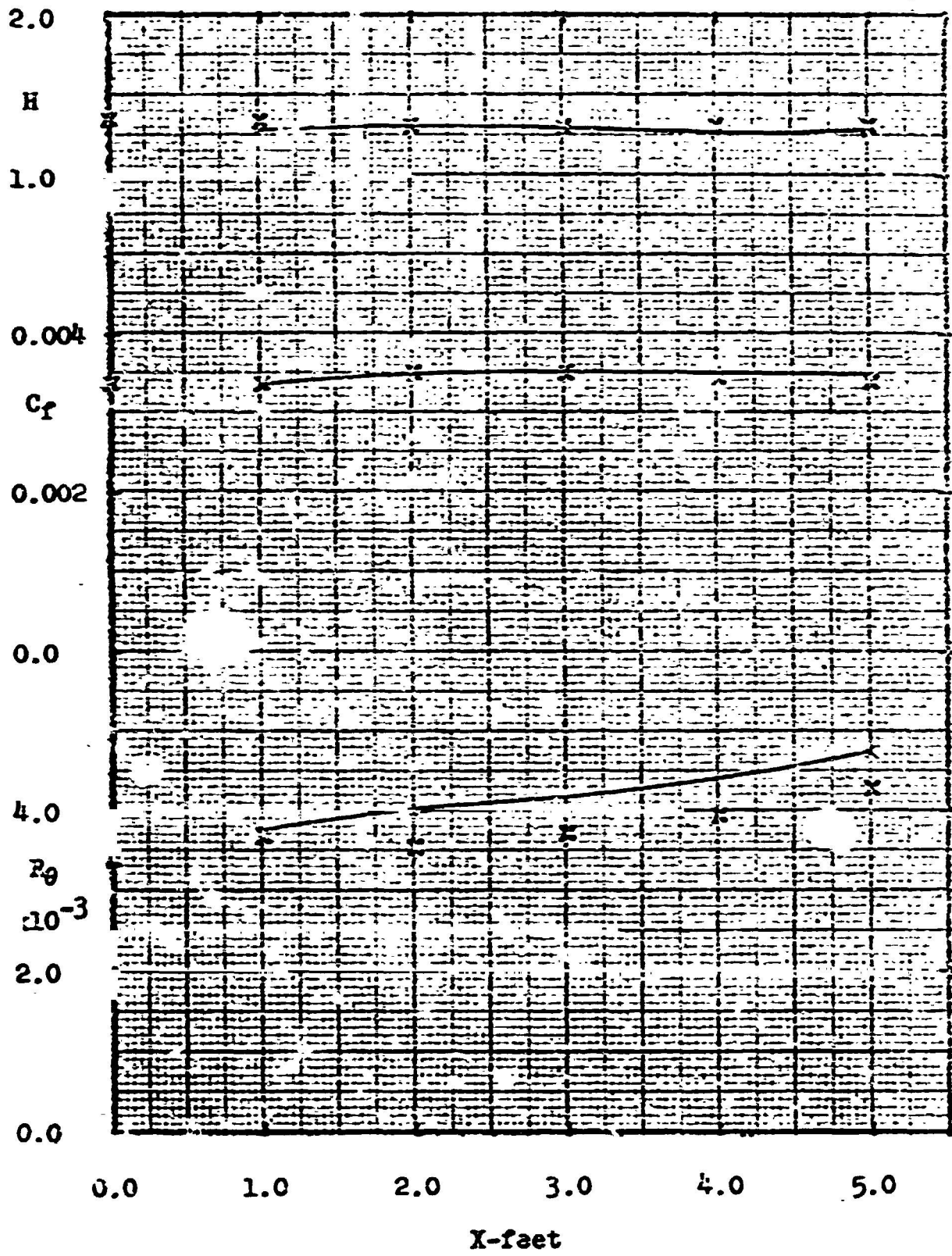
HERRING AND NORBURY $\beta = -0.35$

IDENT= 2700



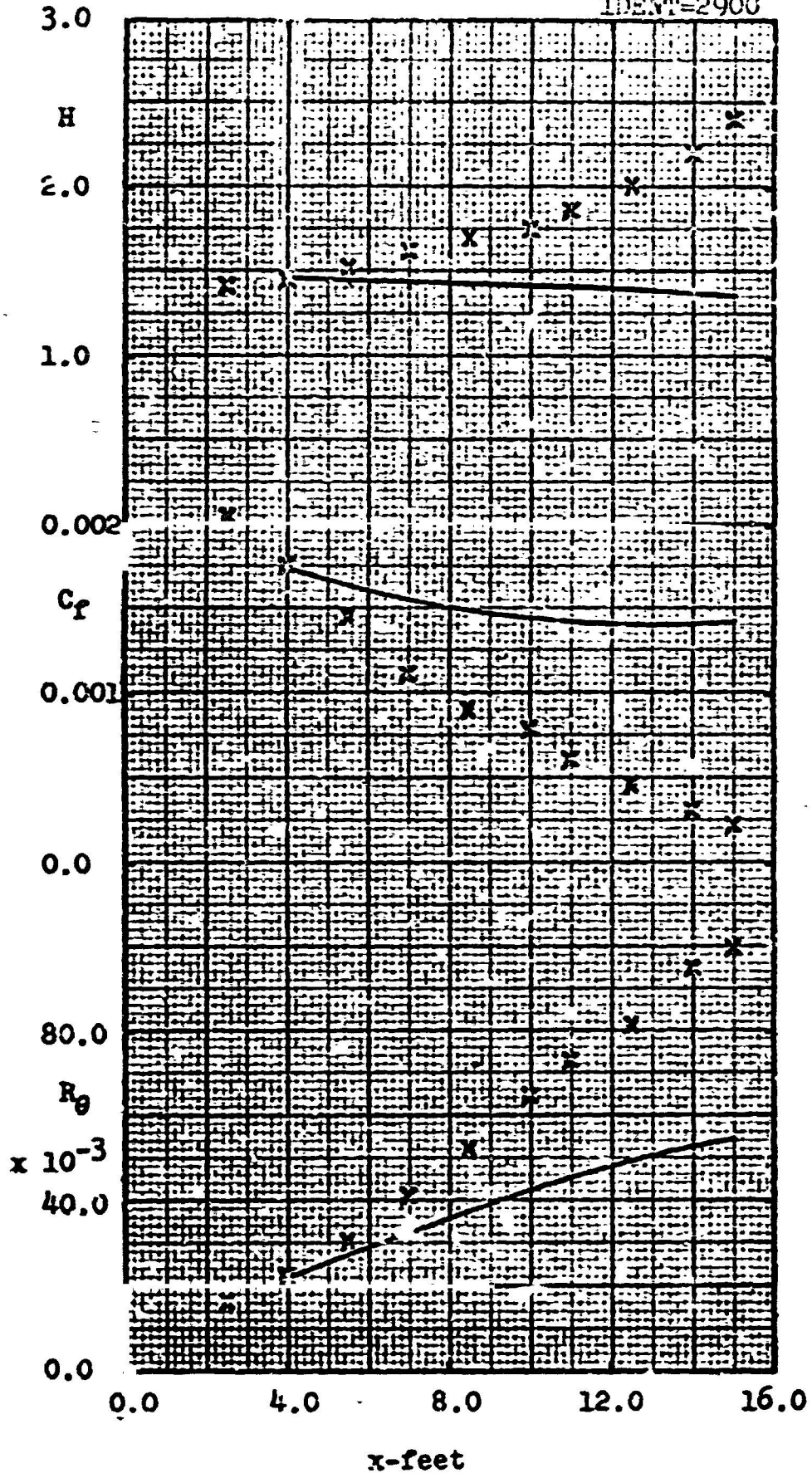
HURE INC AND NORBURY $\beta = -0.35$

IDENT= 2700



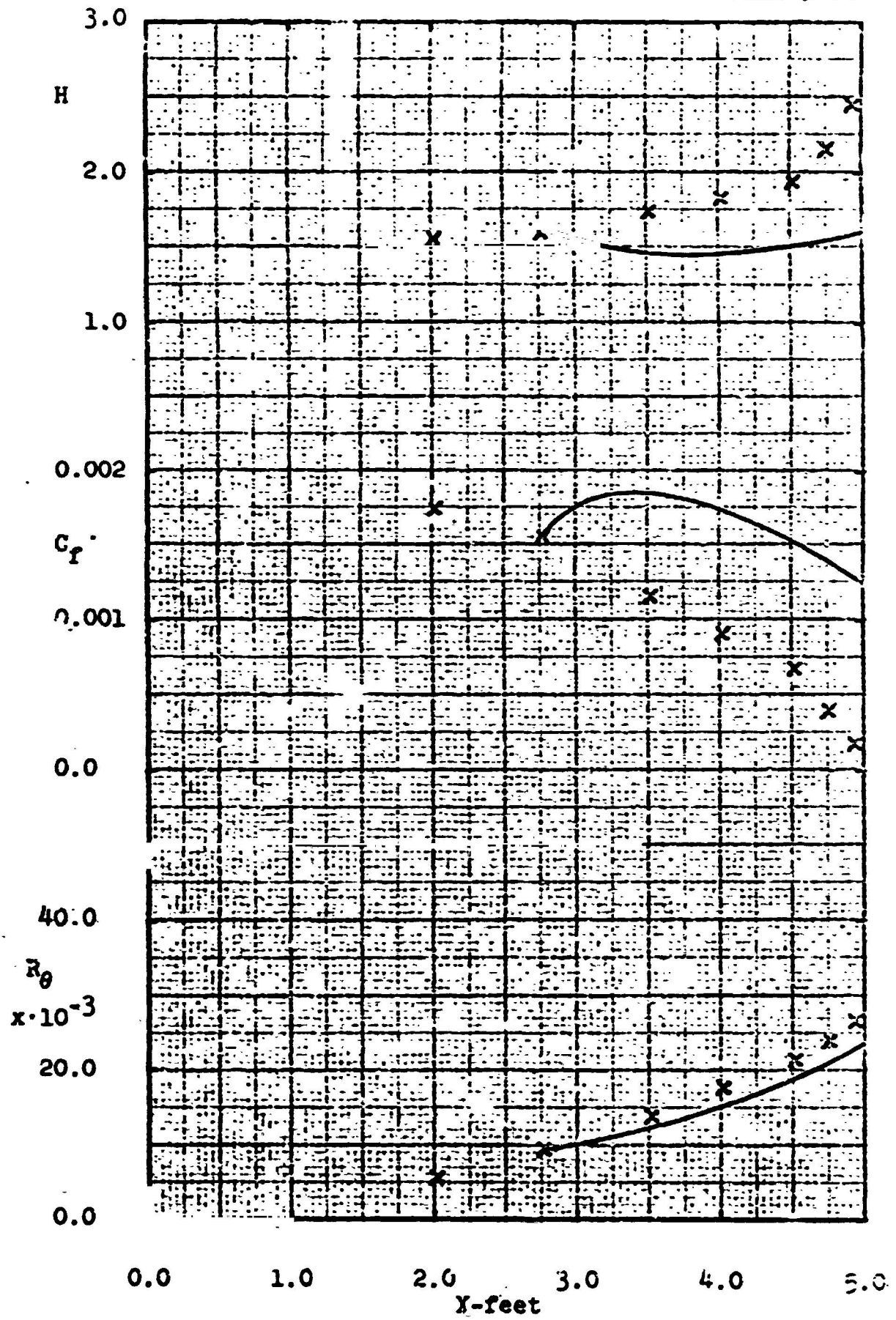
FERRY FLOW

IDENT=2900



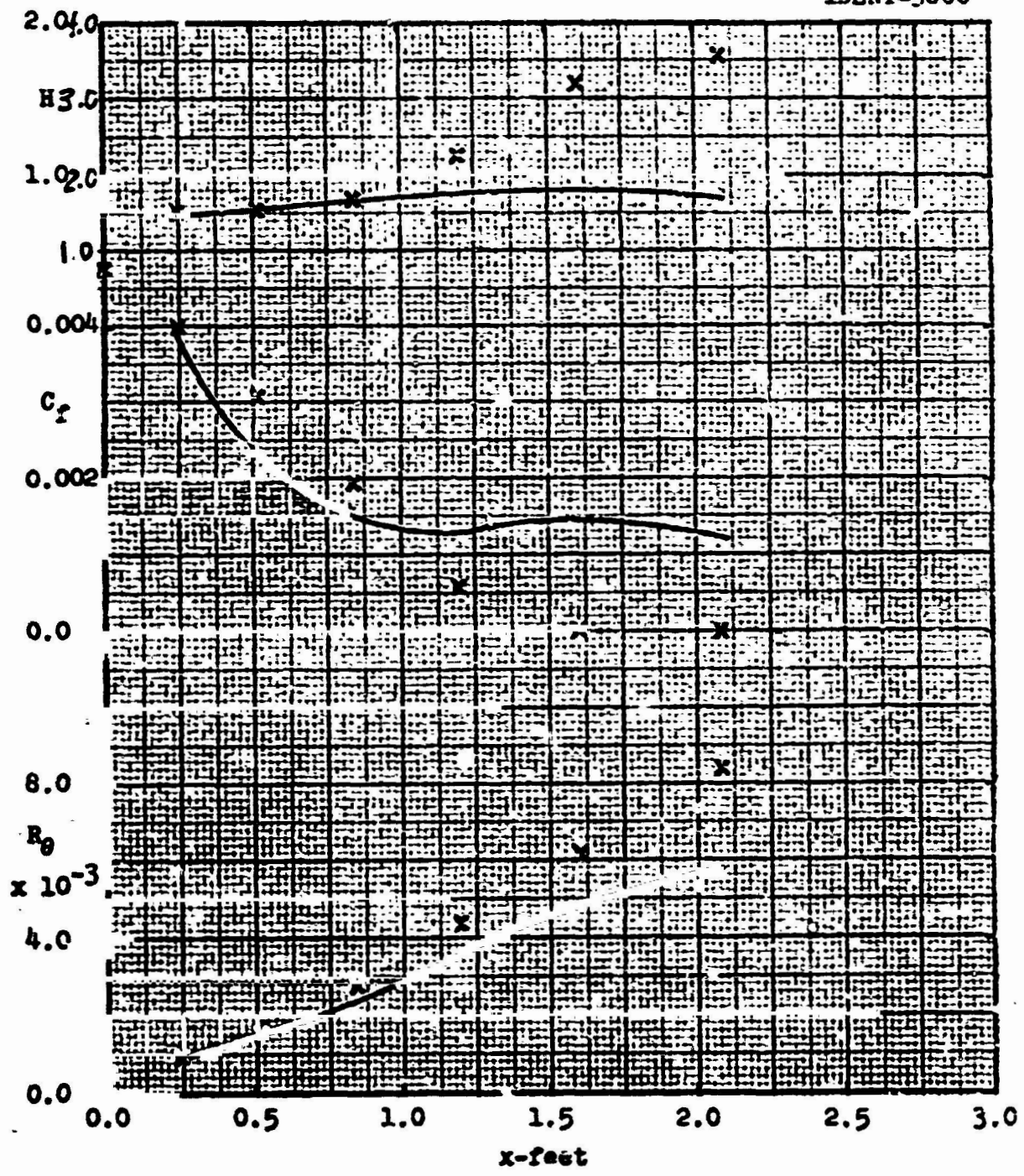
NEWMAN AIRFOIL FLOW - SERIES 2

IDENT=3-00



MOSES CASE 3

IDENT-3800



MOSES CASE 5

IDEN1=4000

